Summer 8-8-2013

Metabolomics Investigation of Glyceollins by On-Line Liquid Chromatography-Electrospray Ionization Tandem Mass Spectrometry and Fungal Metabolite Identification by Thermal Desorption Analysis Coupled with Gas Chromatography-Mass Spectrometry

Syeda Quadri
University of New Orleans, squadri@uno.edu

Metabolomics Investigation of Glyceollins by On-Line Liquid Chromatography-Electrospray Ionization Tandem Mass Spectrometry and Fungal Metabolite Identification by Thermal Desorption Analysis Coupled with Gas Chromatography-Mass Spectrometry

A Dissertation

Submitted to the Graduate Faculty of the
University of New Orleans
in partial fulfillment of the
requirements for the degree of

Doctor of Philosophy
in
Chemistry

by
Syeda Surraiya Quadri

B.S Univeristy of New Orleans, 2007
B.A Univeristy of New Orleans, 2007

August 2013

Dedicated to my parents, Syed M. Hussaini Quadri and Syeda Khalida Quadri

ACKNOWLEDGMENTS

I would like to express my appreciation and gratitude to my research advisor Dr. Richard B. Cole for his support and guidance throughout my graduate studies. His invaluable and innovative ideas motivated me to embark on the field that was very unknown to me. I have gained immense knowledge from his expertise in Mass Spectrometry. His polite attitude and constant encouragement has allowed me to become a confident person. He is truly inspirational and it was a pleasure working under his supervision.

I would like to thank my committee members Dr. Mark L. Trudell, Dr. Mathew A. Tarr, and Dr. Edwin D. Stevens for serving on my committee and all my collaborators, Dr. Robert Stratford, Dr. Mike Ferris, Dr. Jim Cutler, and Dr. Stephen Boue for their helpful suggestions.

Additionally, I would like to acknowledge Bud Schuler. Without his help, I couldn't have started my fungal project. Also, thanks to Harry Rees, Jeff Curry, and Terry Hohenwater for their technical support. I would also like to appreciate my group members, Xiaohua Liu, Dr. Nazim Boutaghou, and Dr. Nalaka Rannulu for all their help throughout the years. It was a pleasure working with them, especially with Nalaka who not only trained me on instruments but also gave me insightful advices. I would also like to thank Phoebe Ray for helping with GC maintenance.

I would like to sincerely thank my parents for their unconditional love, care, and patience. Their tremendous support and faith in me kept me moving forward even at difficult times, and it is because of their prayers that I have come this far. Also, thanks to my loving brothers Moiz,

Muzammil, and Muneem for keeping me entertained at home. I really enjoy spending time with them. Finally, thanks to all my friends, especially the one who have always been there for me.

TABLE OF CONTENTS

LIST OF FIGURES

LIST OF SCHEMES

LIST OF TABLES

ABSTRACT

Metabolomics is an emerging field that entails the detailed characterization of the ensemble of metabolites produced by living organisms; subfields include drug metabolism and natural environmental toxin production. The first part of the dissertation pursued metabolism of glyceollins, i.e., isoflavones produced by soybeans that are potential cancer therapy agents. *In vivo* glyceollin metabolites produced in rats were investigated by on-line Liquid Chromatography-Electrospray Ionization Tandem Mass Spectrometry. An odd-electron fragment ion at m/z 148, formed in violation of the even-electron rule, and diagnostic of the glyceollin backbone, was discovered. Based on this finding, a negative mode precursor ion scanning method was developed to screen for glyceollins and their metabolites from biological samples. Products of both Phase I and Phase II metabolism were identified, none of which have been previously reported. Sulfated metabolites were confirmed by accurate mass measurement, while glucuronide conjugation was confirmed by enzyme-assisted glucuronidation by rat liver microsomes. Intact GSH-glyceollin conjugates were not observed, but breakdown products of the GSH pathway, i.e., cysteinylglyceine, cysteine, and acetylated cysteine, were identified as conjugates of oxygenated glyceollins. The identification of GSH by-product conjugates was confirmed in product ion spectra acquired in the negative mode (where peptide anions, and glyceollin-bearing cleaved peptide portions were observed), as well as in the positive mode (where intact oxygenated glyceollin fragments appeared without the initially-present peptide portion). Mass spectral evidence strongly

supports a metabolic pathway involving initial epoxidation of glyceollins followed by GSH addition at the epoxidation site.

The second part of the dissertation undertook the investigation of secondary metabolites called microbial volatile organic compounds (MVOCs) produced by fungi (mold) that have been reported to have adverse human health effects. MVOCs were collected onto different sorbent materials and analyzed by Thermal Desorption Analysis coupled with on-line Gas Chromatography-Mass Spectrometry. Fungal MVOCs were characterized from various simulated flooding conditions (brackish, freshwater, and saltwater) and different substrates (nutrient rich vs. low nutrient) to determine diagnostic MVOCs. Ten fungi from simulated environments were identified by genetic sequencing. *Cladosporium sp.* and *Chaetomium sp.* were cultivated and their emitted MVOCs, 3-furaldehyde and 3-(4-hydroxy-3-methoxyphenyl)-2-propenal, were proposed as diagnostic indicators of these fungi.

CHAPTER 1

SCREENING AND IDENTIFICATIN OF GLYCEOLLINS AND THEIR METABOLITES BY ELECTROSPRAY IONIZATION TANDEM MASS SPECTROMETRY WITH PRECURSOR ION SCANNING

Syeda S. Quadri, Robert E. Stratford, Stephen M. Boué, and Richard B. Cole

1.1 Abstract

A method has been developed for screening glyceollins and their metabolites based upon precursor ion scanning. Under higher-energy collision conditions employing a triple quadrupole mass spectrometer in the negative ion mode, deprotonated glyceollin precursors yield a diagnostic radical product ion at *m/z* 148. We propose this resonance-stabilized radical anion, formed in violation of the even-electron rule, to be diagnostic of glyceollins and glyceollin metabolites. Liquid chromatography-electrospray ionization tandem mass spectrometry (LC-ESI-MS/MS) established that scanning for precursors of *m/z* 148 can identify glyceollins and their metabolites from plasma samples originating from rats dosed with glyceollins. Precursor peaks of interest were found at *m/z* 337, 353, 355, 417, and 433. The peak at *m/z* 337 corresponds to deprotonated glyceollins, whereas the others represent metabolites of glyceollins. Accurate mass measurement confirmed *m/z* 417 to be a sulfated metabolite of glyceollins. The peak at *m/z* 433 is also sulfated, but it contains an additional oxygen, as confirmed by accurate mass measurement. The latter metabolite differs from the former likely by the replacement of a hydrogen with a hydroxyl moiety. The peaks at *m/z* 353 and 355 are proposed to correspond to hydroxylated metabolites of glyceollins wherein the latter additionally undergoes a double bond reduction.

1.2 Introduction

Soybean produces isoflavones that are known to have beneficial effects on human health.[1,2,3,4,5] In recent years, much research has been conducted on genistein, an isoflavone that has been proposed to have anti-cancer activity.[6,7,8] The potential chemopreventive effect of genistein has prompted researchers to investigate soybean further for anticancer agents. A more recently investigated type of isoflavones are the glyceollins that are produced by soybeans under stressed conditions. The stressful conditions may include exposure to UV light, or fungal (e.g., *Aspergillus*) or bacterial pathogens.[9] Because they are produced by a defense mechanism in response to pathogen invasion, glyceollins may be referred to as phytoalexins.[10]

Glyceollins exist in three isomeric forms, Glyceollin I, II and III (Scheme 1.1). The isomers are derived from a daidzein precursor through several intermediate steps.[11] Among the biological effects of glyceollins are potential human health benefits including anti-fungal, anti-oxidant, anti-inflammatory, anti-diabetic, and cancer cell anti-proliferative activity along with other beneficial properties.[12,13,14] Recently, many studies have proposed glyceollins as prevention or therapy candidates for breast, ovarian, and prostate cancers. All three glyceollin isomers have exhibited anti-estrogenic effects on estrogen receptor function and estrogen-dependent tumor growth. [15, 16] Specifically, glyceollins bind to the estrogen receptor and they inhibit estrogen-induced tumor progression of breast cancer (MCF-7) and ovarian cancer (BG-1) cells.[16] Among the three isomers, glyceollin I has the most potent anti-estrogenic activity.[17,18] Another *in vivo* study examining post-menopausal monkeys suggested glyceollins reduce breast cancer biomarker expression.[19] Human prostate cancer cell research demonstrated that glyceollins have multiple effects on prostate cancer cells (LNCaP).[20]

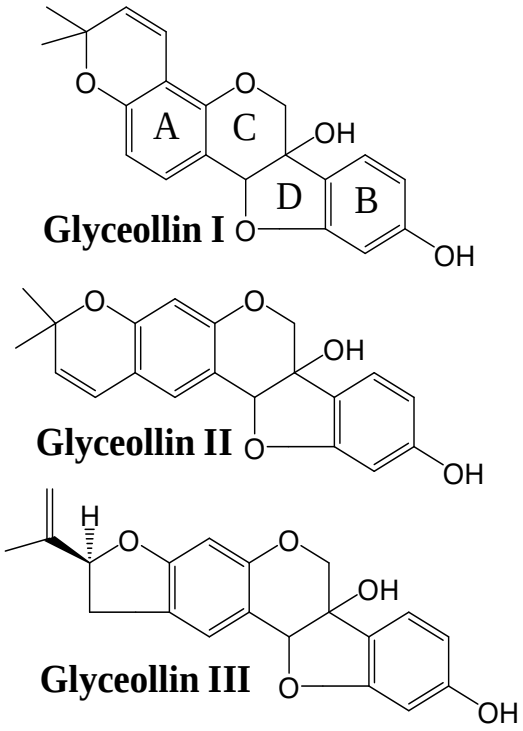

Scheme 1.1: Structures of Glyceollin isomers

The inhibition of prostate cancer cell growth by glyceollins is similar to that exhibited by genistein, but the former also up-regulate cyclin-dependent kinase inhibitor and down-regulate mRNA levels for androgen-responsive genes through androgen-mediated pathways.[20] In addition to the anti-estrogenic activity, glyceollins normalize glucose homeostasis and improve glucose utilization in adipocytes.[13,21] The anti-diabetic potential was also noted in prediabetic[21] and Type 2 diabetic rats[21] and mice.[22] These potential benefits of glyceollins have been well documented, but its metabolism is not well understood.[23]

Several mass spectrometric approaches that use various ionization techniques such as electron ionization (EI), fast atom bombardment (FAB), thermospray (TSP), atmospheric pressure chemical ionization (APCI), and electrospray ionization (ESI) have been used to investigate flavonoids.[24,25,26,27,28] Tandem mass spectrometry using low-energy collision-induced dissociation

(CID) to obtain structural information regarding mass-selected precursors has been shown to be advantageous in characterizing flavonoids[28] and was recently applied in the analysis of glyceollins from soy bean extracts.[29] Given the propensity for extensive metabolism of flavonoids following their ingestion[30] and that no research has addressed identification of glyceollins' metabolites in animal systems, the significance of the present research is that it investigates glyceollins in plasma and presents method development work designed for screening of glyceollins and glyceollin-related metabolites.

1.3 Experimental Methods

1.3.1 *Extraction of Glyceollins isomers*

A mixture of glyceollins I, II, and III was obtained using a procedure developed at the Southern Regional Research Center (ARS, USDA, New Orleans, LA). Briefly, soybean seeds (1 kg) were sliced and inoculated with *Aspergillus sojae*. After 3 days, the glyceollins were extracted from the inoculated seeds with 1 L methanol (Aldrich Chemical Co., St. Louis, MO). The glyceollins were isolated using preparative scale HPLC using two Waters (Milford, MA) 25 x 100 mm, 10 µm particle size µBondapak C_{18} radial compression column segments that were combined using an extension tube. HPLC was performed on a Waters 600E System Controller combined with a Waters UV-Vis 996 detector scanning from 210-400 nm. Elution was carried out at a flow rate of 8.0 mL/min with the following solvent system: A = acetonitrile (Aldrich Chemical Co.), B = water (Millipore system, Billerica, MA) 5% A for 10 min, then 5% A to 90% A in 60 min followed by holding at 90% A for 20 min. The injection volume was 20 mL. The fraction containing the glyceollins was concentrated under vacuum and freeze-dried. Confirmation of individual glyceollins was based on matching of HPLC retention times and matching of UV-Vis absorbance spectra with those of authentic standards isolated at SRRC[17]. UV-Vis spectrophotometry at 285 nm allowed an estimation of mixture contents used in all experiments: glyceollin I (68%), glyceollin II (21%), and glyceollin III (11%).

1.3.2 *Glyceollin dosing of rats and plasma sample collection*

The administration of glyceollins to rats and subsequent sample collection have been previously described.[21] Briefly, glyceollins were dissolved in poloxamer to administer 90 mg/kg via oral gavage (3 mL) to male ZDSD rats (PreClinOmics, Indianapolis, IN) that were housed in a suspended wire cage and maintained on a 12:12 hr light-dark cycle. Three hr after administration,

rats (approx. 500 g wt.) were euthanized at various time points by decapitation and trunk blood was collected into EDTA-coated tubes supplemented with aprotinin. Plasma was separated and stored at -80 ºC until analysis. Glyceollins were extracted for mass spectrometry analysis by thawing the samples and transferring 125 µL of plasma into a microcentrifuge tubes. An equivalent volume of acetonitrile was then added. The mixture was vortexed and centrifuged at 10,000 rpm for 20 min. 100 µL of supernatant was transferred into a clean microcentrifuge tube for analysis.

1.3.3 *Liquid Chromatography-Mass Spectrometry*

LC-MS and LC-MS/MS analyses were conducted on an Agilent 1200 series LC system (Agilent, Santa Clara, CA) coupled with a 3200 QTrap triple quadrupole mass spectrometer (Applied Biosystems/MDS SCIEX, Foster, City, CA). Separation was performed on an Agilent Eclipse - XDB C18 column (4.6 x 150 mm ID, 5 µm). 10 µL was injected onto the column held at 25 ºC. Mobile phase A was water with 0.1% formic acid whereas mobile phase B was acetonitrile with 0.1% formic acid. The gradient was 0-2 min 3% B, 2-7 min 3% to 60% B, 7-14 min 60% to 100% B, 14-20 min 100% B, 20-30 min 100% to 3% B. Flow rate was 0.500 mL/min. The UV absorbance detector was set at 210 and 282 nm.

All mass spectrometry experiments were performed in the negative ion mode. For LC-ESI-MS and LC-ESI-MS/MS analyses, electrospray parameters were set at: curtain gas 10 psi, ionspray voltage -4000 V, GAS1 60 psi, GAS2 60 psi, source temperature 600 ºC, CAD gas pressure 6 psi, entrance potential -10 V, collision cell exit potential -3 V. Declustering potential and collision energy were optimized to be -75 V and -34 eV, respectively. The information-dependent acquisition (IDA) method was employed to perform full scan, tandem MS and precursor ion scans sequentially (1 sec/scan).

1.3.4 Direct Infustion ESI-MS

Direct infusion parameters were the same as above except for GAS1, GAS2 and source temperature, which were set at 20 psi, 0 psi, and 50 ^{o}C, respectively. Samples were infused for 2 min at a flow rate of 4 µL/min. Direct infusion data was acquired using multiple-channel acquisition (MCA).

1.3.5 Accurate mass measurements by ESI-FRICR-MS

Accurate mass measurements to determine metabolite empirical formulas were performed on a Solarix 7T fourier transform ion cyclotron resonance (FT-ICR) mass spectrometer (Bruker Daltonics, Bremen, Germany). An ESI voltage of 4500 V was used with 2 Bar nebulizer gas pressure; drying gas was delivered at 4 L/min and 200 °C drying temperature. Peaks at m/z 113, 432, and 602 from ESI Tuning Mix (Agilent Technologies, Santa Clara, CA) were used as internal standards in mass spectra consisting of 40 averaged acquisitions.

1.4 Results and Discussion

1.4.1 *Collision-Induced Dissociations of Glyceollins*

Isomeric glyceollin I, II, and III standards and plasma samples obtained from rats dosed with glyceollins were analyzed and characterized by negative ion MS and tandem MS. $[M-H]^-$ peaks corresponding to deprotonated forms of glyceollin isomers were observed at *m/z* 337. Low-energy CID of these $[M-H]^-$ precursors (Figure 1-1) produced product ion peaks similar to those reported by Gruppen et al.[29] For instance, *m/z* 319, 215, 187, 175, 161, 149 were all present in high abundances. In addition, low abundance peaks reported by Gruppen et al.[29] (*m/z* 322, 309, and 293) were also observed. Surprisingly, under higher-energy conditions in the negative ion mode, a previously unreported CID peak emerged at *m/z* 148 with such a strong signal that it became the base peak in the product ion spectrum (Figure 1-1).[31] We attribute the dominance of this open-shell fragment in the product ion mass spectrum of glyceollins to its exceptional stability as supported by the extensive delocalization of both the charge and the radical over the aromatic ring system (see inset, Figure 1-1). Indeed, fragmentation to form this product constitutes a violation of the even-electron rule,[32] i.e., normally formation of a radical product ion plus a radical neutral is forbidden from decompositions of an even-electron precursor. However, homolytic cleavage of even-electron ions has been documented to occur especially in cases where exceptional stability is acquired by the formed radical ion and radical neutral. [32,33,34,35] Because the *m/z* 148 product ion is formed from the portion of the molecule that is conserved in all of the glyceollin isomers, we propose to use the appearance of this unique radical ion in MS/MS spectra as a product ion diagnostic of all glyceollins.[31] Thus, the presence of this product ion can be used as a signature to identify glyceollins and their related metabolites. As a single caveat, in cases where the D or B rings become modified, the *m/z* 148 ion could be shifted to another even *m/z* value with a possible

decrease in intensity. Notably, this product ion was also observed during low-energy sustained off-resonance irradiation (SORI) - CID in a FT-ICR. The empirical formula ($C_8H_4O_3$) of the resonance stabilized m/z 148 ion was confirmed by accurate mass measurement.

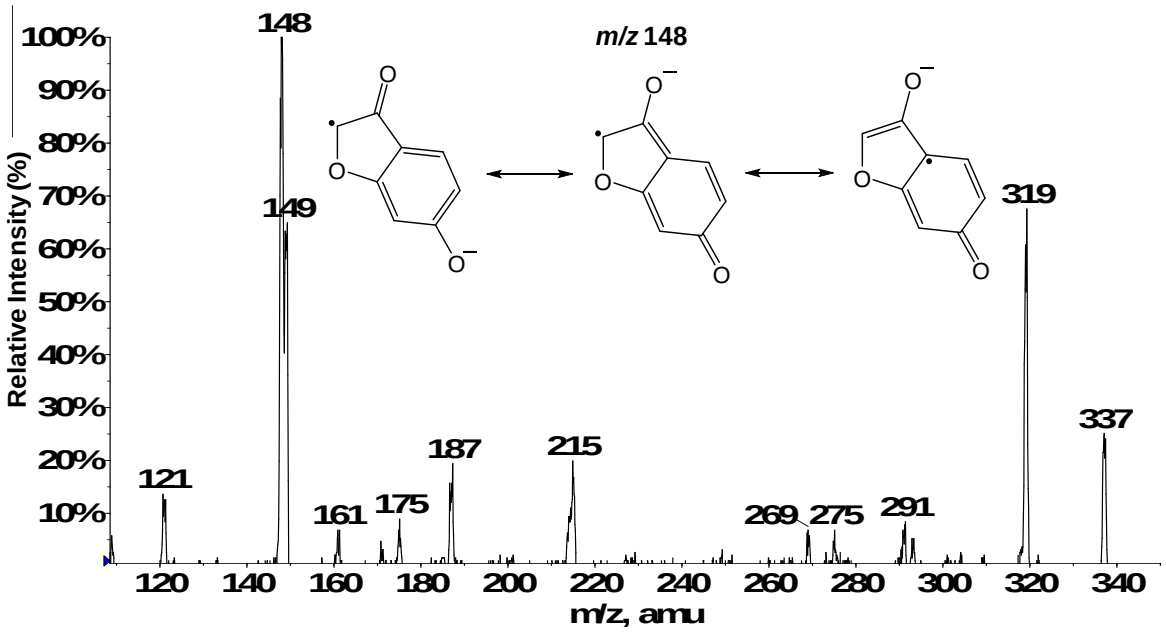

Figure 1-1: Negative ion electrospray product ion mass spectrum (-75 eV CID) of $[M-H]^-$ precursor of glyceollin (*m/z* 337). Under these higher-energy conditions, the product ion at *m/z* 148 appears in high abundance.

1.4.2 *Optimization of CID conditions*

CID conditions for the triple quadrupole, including the "declustering potential" (V, also known as nozzle-skimmer potential) and the collision energy (eV, E_{lab}) were serially adjusted to maximize the intensity of the diagnostic product ion at *m/z* 148 formed from glyceollin $[M-H]^-$ precursors. Other MS conditions such as ion spray voltage, curtain, nebulizing and turbo gases were maintained at constant values (see Experimental section). The declustering potential value for precursor *m/z* 337 was optimized (by ramping up its voltage) to obtain the highest intensity of *m/z* 148 in product ion mode. The optimum declustering potential yielding the maximum intensity of *m/z* 148 was -75 V. Tandem MS of *m/z* 337 was then performed using a fixed declustering potential of -75 V, while ramping up the collision energy. The highest signal for *m/z* 148 was observed at an E_{lab} value of -34 eV. Figure 1-2 shows the automated infusion "quantitative optimization" of the declustering potential (Figure 1-2a, *m/z* 148 only) and E_{lab} (Figure 1-2b, 3 highest intensity fragments: *m/z* 148, *m/z* 149 and *m/z* 319). The breakdown curves shown in Figure 1-2b clearly indicate that upon decomposition of *m/z* 337, *m/z* 149 has a lower appearance energy than *m/z* 148. This finding can be rationalized by considering that for these closely related fragments, production of even-electron *m/z* 149 (with formation of an additional carbon-hydrogen bond and resulting stabilization) requires less energy than formation of odd- electron *m/z* 148. However, as the internal energy uptake is increased, the rate constant of *m/z* 148 formation becomes more favorable and the curves for formation of the respective products cross (Figure 1-2b inset). This curve-crossing is a classic example[36,37] of competitive ion formation where the fragment with the lower appearance threshold dominates under lower energy collisions (e.g., conditions used by Gruppen *et al.*[29], *m/z* 149 is favored), whereas the fragment formed by the higher frequency factor[32] process dominates at higher collision energies (*m/z* 148, see Figure 1-1).

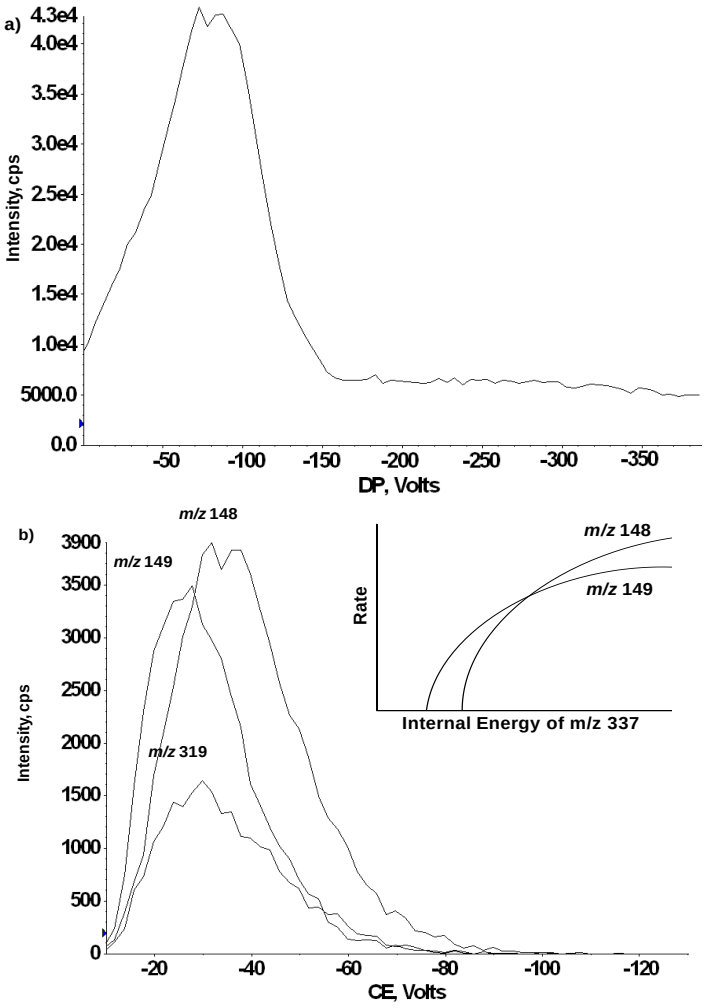

Figure 1-2: (a) The optimum declustering potential value to produce *m/z* 148 from CID of *m/z* 337 precursors was determined by ramping the declustering potential in product ion mode. The maximum intensity of *m/z* 148 was observed at -75 V. (b) Optimization of collision energy for *m/z* product ion formation at fixed declustering potential of -75 V. Abundances of three strong peaks: *m/z* 148, 149, 319 are shown as a function of collision energy. The highest signal for *m/z* 148 was observed at -34 eV (E_{lab}). The inset schematically shows the rates of formation of *m/z* 148 and 149 as a function of internal energy of *m/z* 337.

1.4.3 Precursor Ion Scan of m/z 148

Upon optimization of CID conditions, *m/z* 148 was observed as the base peak in the product ion mass spectra of $[M-H]^-$ precursors from each purified standard of glyceollin I, II, and III. To follow through on the idea of using *m/z* 148 as a diagnostic product ion for glyceollins, the above optimized CID conditions maximizing *m/z* 148 production were used to obtain precursor ion scans of *m/z* 148 using glyceollin mixtures. As expected, $[M-H]^-$ at *m/z* 337 was detected in high intensity, thus confirming that precursor ion scans of the diagnostic radical *m/z* 148 can be used to detect glyceollins and glyceollin related compounds. In principle, one could also consider using m/z 149 for precursor ion scans, but in practice, this would be a poor choice because a wide variety of phtahlate esters (ubiquitous plasticizers) produce m/z 149 upon ESI-MS/MS.[38]

1.4.4 LC-ESI-MS and LC-ESI-MS/MS analyses of glyceollins and their metabolites in rat plasma

To test the validity of this method to identify glyceollins and their metabolites, it was applied to the analysis of plasma samples derived from rats dosed with glyceollins. For these LC-ESI-MS and LC-ESI-MS/MS experiments, the MS data acquisition method cycled through a full MS scan, a CID precursor ion scan of *m/z* 148, and a CID product ion spectrum of *m/z* 337. Once the precursors of *m/z* 148 were identified, in subsequent runs, the CID product ion scans of those precursors were added to the acquisition scan cycle. In a plasma sample taken at 20 min following a 90 mg/kg dose of glyceollins, the precursor ion scan of *m/z* 148 showed eluting peaks at 10.5 and 12.5 min (Figure 1-3a). The peak at 12.5 min corresponds to (unmetabolized) deprotonated glyceollins (*m/z* 337) as shown in the averaged mass spectrum corresponding to this chromatographic peak (Figure 1-3 inset). The earlier eluting peak (10.5 min) corresponds to an

apparent metabolite of glyceollins which gave a base peak at *m/z* 417 (Figure 1-3 inset). Notably, the employed CID conditions produced enough internal energy uptake to cause consecutive decomposition of this metabolite to produce *m/z* 337 (deprotonated glyceollins). In a different rat plasma sample taken at 4 hrs following the dose of glyceollins (90 mg/kg), precursor ion scanning of *m/z* 148 resulted in the appearance of glyceollin metabolites eluting at 3.9, 4.2 and 9.6 min (Figure 1-4). These chromatographic peaks correspond to metabolites of *m/z* 451, 433, and 417, respectively (see inset Figure 1-4). Again, consecutive decomposition of the *m/z* 417 metabolite was observed to produce *m/z* 337. It appears that metabolism was extensive in this case because unmodified glyceollins were not detected in this sample.

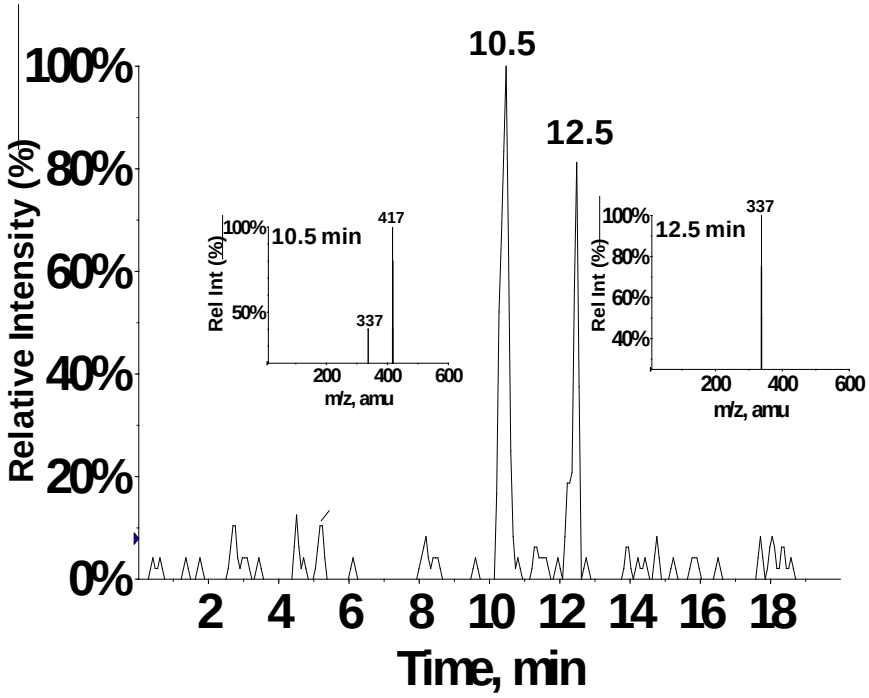

Figure 1-3: LC-MS/MS precursor ion scans showing total ion current of all precursors of *m/z* 148 from glyceollins dosed rats. The insets show the precursor ion spectra of *m/z* 148 averaged over the width of the peaks eluting at 10.5 and 12.5 min showing the presence of a metabolite and unmetabolized glyceollins, respectively.

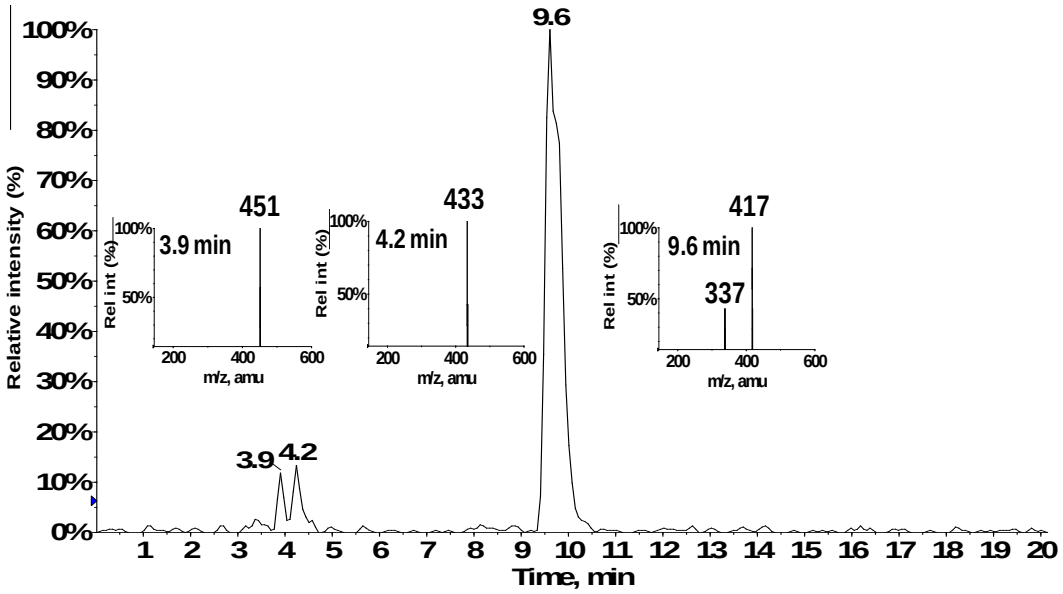

Figure 1-4: LC-MS/MS precursor ion scan showing total ion current of all precursors of *m/z* 148 from glyceollins dosed rat plasma. Inset are the averaged mass spectra obtained across the three observed chromatographic peaks.

1.4.5 Identification of glyceollins' metabolites using LC-ESI-MS and LC-ESI-MS/MS

The CID product ion spectrum of the *m/z* 417 precursor (Figure 1-5) shows many of the same fragments as observed in the CID product ion spectrum of *m/z* 337 (Figure 1-1). In considering the mass increase of this metabolite, in general, an addition of 80 Da in a biological medium may correspond to either a sulfation or a phosphorylation process. The metabolism of glyceollins in the digestive tract is not well documented[23] and to our knowledge there have not been any reports of glyceollins' metabolites. However, another isoflavone, genistein, has been extensively studied, and it has been reported to undergo phase II metabolism by glucuronidation, sulfation, and methylation in small intestine and liver.[30,39,40] Based on these reports of genistein metabolism, and interpretation of the obtained CID spectrum of *m/z* 417 (Figure 1-5), the peak was tentatively assigned as the sulfated metabolite of glyceollins. However, because *m/z* 417 could correspond to either the sulfated or the phosphorylated metabolite (deprotonated forms), to

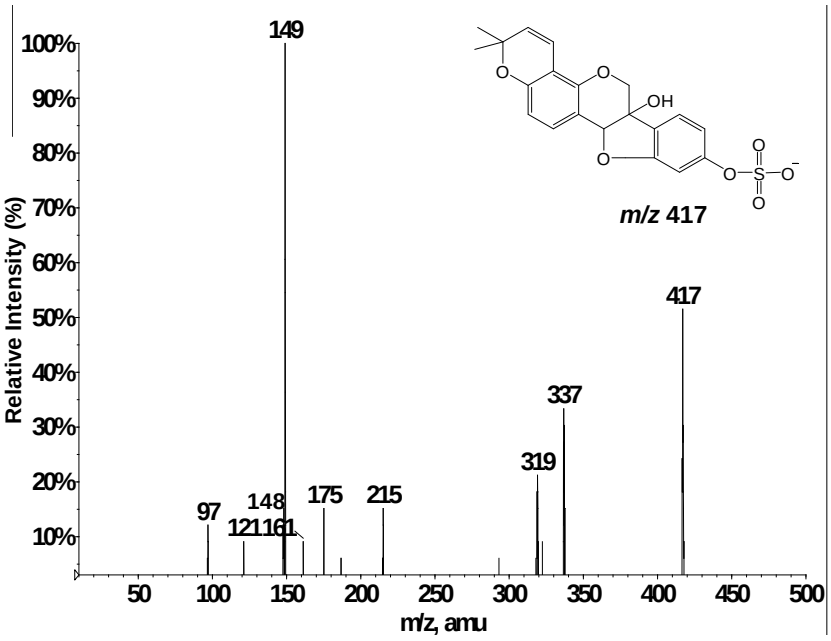

Figure 1-5: LC-MS/MS product ion mass spectrum of *m/z* 417 precursors from rats dosed with glyceollins. The *m/z* 417 metabolite was assigned as a sulfated form of glyceollins.

definitively identify *m/z* 417, accurate mass analysis was performed on this ion. The addition of a phosphate group implies a molecular formula of $C_{20}H_{18}O_8P$ with an exact *m/z* of 417.074478, whereas sulfated glyceollins have the molecular formula $C_{20}H_{17}O_8S$ with an exact *m/z* of 417.064962. The accurate mass measurement by FT-ICR gave *m/z* 417.064812 confirming the assignment of *m/z* 417 as a sulfated metabolite of glyceollins (0.360 ppm error). Because the CID product ion spectrum of *m/z* 417 (Figure 1-5) shows similar fragments as the CID product ion spectrum of *m/z* 337 (Figure 1-1), and because there are no fragment ions that are shifted by 80 *m/z* units in the former spectrum relative to the latter, we conclude that the sulfate group is the most labile moiety of the *m/z* 417 metabolite. Thus, the first step in decompostion of *m/z* 417 is loss of SO_3 neutral to form deprotonated glyceollins at *m/z* 337. All of the lower *m/z* fragments in Figure 1-5 are proposed to be formed by consecutive decompositions of *m/z* 337. Notably, at the constant E_{lab} collision energy (- 34 eV) employed throughout this paper, energy is consumed in

the decomposition of *m/z* 417 leading to *m/z* 337. The m/z 337 ions thereby formed have less internal energy available to induce consecutive decompositions as compared to *m/z* 337 precursors that are subjected directly to -34 eV collisions in the central quadrupole. This loss of internal energy in the first step of decomposition results in more favorable kinetics for *m/z* 149 formation as compared to *m/z* 148 (see Figure 1-2b inset) in consecutive decompositions.

The hydroxyl sites of glyceollins are preferred sites of sulfation. We assign sulfation to the hydroxyl site of the phenol group (see inset, Figure 1-5) based upon the observed facile loss of SO_3 neutral which, in this case, leaves a resonance stabilized phenoxy anion (corresponding to deprotonated glyceollins at *m/z* 337). The loss of SO_3 neutral from glyceollins sulfated at the alkyl hydroxide would be expected to be less favorable. As glyceollins are known to exhibit competitive behavior with estrogens, this assignment is supported by the documented preferential sulfation of the 3-phenolic hydroxyl relative to the 16-aliphatic hydroxyl in estriol.[41]

Another metabolite appearing in Figure 1-4 (retention time 4.2 min corresponding to *m/z* 433) was investigated further. The composition of *m/z* 433 was established to be $C_{20}H_{17}O_9S$ by accurate mass measurement (*m/z* 433.059649, 0.524 ppm error). This peak at *m/z* 433 is proposed to correspond to a (deprotonated) sulfated metabolite of glyceollins that contains one additional oxygen relative to *m/z* 417 discussed above. The LC-ESI-MS/MS low-energy CID product ion spectrum of the *m/z* 433 precursor (Figure 1-6) reveals the B fragment peaks (*m/z* 148, 149) to be the same as those in the product ion spectrum of deprotonated glyceollins (*m/z* 337, Figure 1-1) whereas A fragments are shifted by 16 *m/z* units (i.e., *m/z* 175 and 227 are shifted to 191 and 243, respectively), plus *m/z* 337 is shifted to 353. This different behavior of A and B fragments allows us to narrow down the potential sites of hydrogen replacement with a hydroxyl group that accounts

for the 16 Da shift in the mass of the metabolized molecule. All possible hydroxylation sites are marked with asterisks on the structure of *m/z* 433 shown in Figure 1-6.

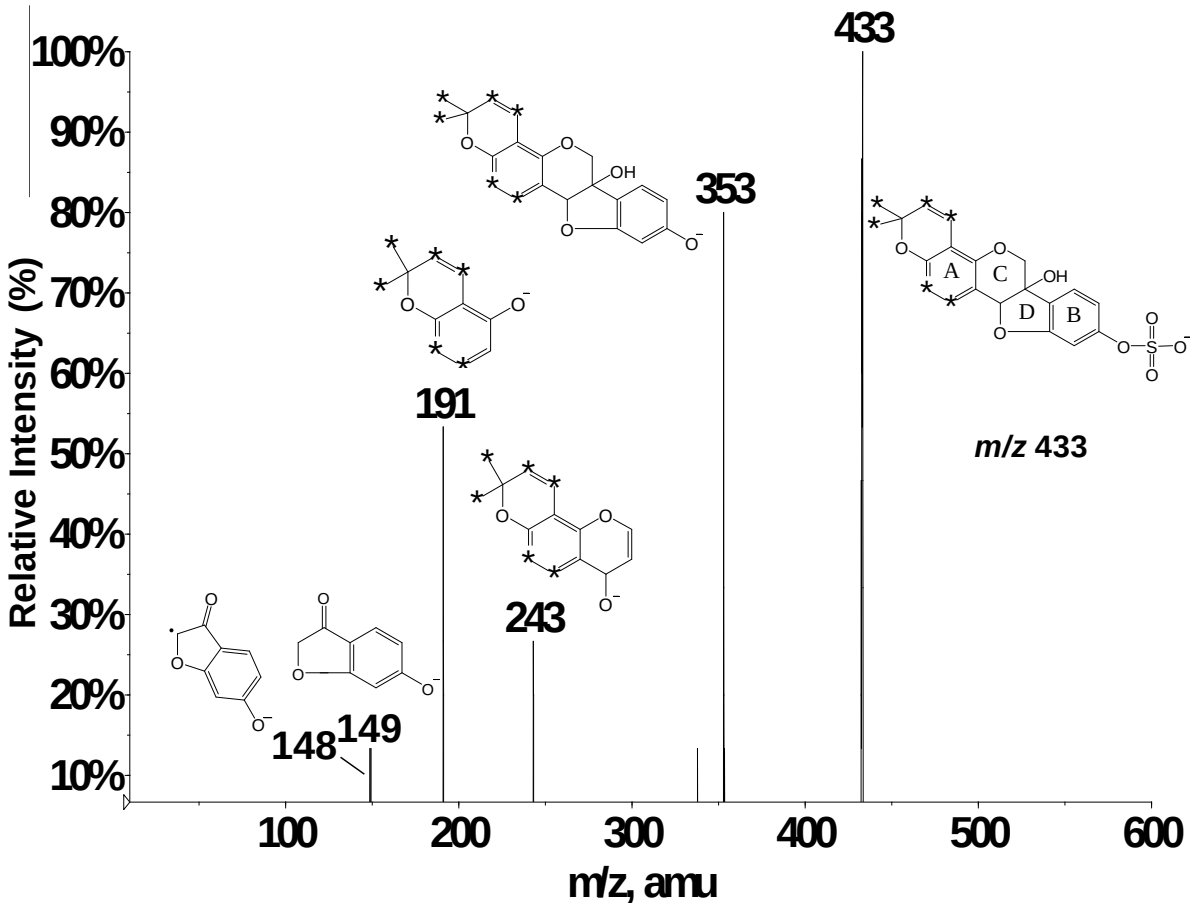

Figure 1-6: Negative ion low-energy CID product ion mass spectrum of *m/z* 433 from rats dosed with glyceollins. Potential sites of replacement of a hydrogen with a hydroxyl group are marked with asterisks. The labeling of the ring system has been adopted from Gruppen *et al*.[29]

1.4.6 Screening of glyceollins' metabolites by direct infusion

LC separation prior to ESI-MS or ESI-MS/MS analyses offers the theoretical advantage that each analyte species may enter the ESI source of the mass spectrometer free from interferences. Even so, the sequential isolation and analysis steps of tandem mass spectrometry can enable direct mixture analyses in the absence of chromatographic separation. When very complex mixtures are under investigation, however, analyte desorption behavior may be affected by competing sample species. It is well documented that in ESI-MS, surface-active species tend to be desorbed most efficiently, whereas the less surface-active molecules tend to experience signal suppression.[42] To compare the performance of our precursor ion scanning approach in the presence and absence of chromatographic separation, the same rat plasma mixture as used above was employed, except that this time precursor ion scans of *m/z* 148 were performed directly on the complex mixture with no prior LC separation. Direct infusion of the acetonitrile extracts of a rat plasma mixture resulted in the detection of *m/z* 148 precursor ions at *m/z* 337, 353, 355, 417, 433, 451, and 469 (Figure 1-7). The peak at *m/z* 337 once again represents unmetabolized deprotonated glyceollins. The peaks at *m/z* 417 and 433 were previously assigned as the sulfated metabolite of glyceollins, and the sulfated metabolite of glyceollins with one additional oxygen, respectively. It is fair to say that neither the *m/z* 417 nor the *m/z* 433 signal was suppressed during ESI-MS/MS direct mixture analysis. This may be rationalized by considering that the sulfated conjugates of glyceollins have substantial surfactant character, which can explain the favorable signal response relative to other components of the complex mixture.

Notably, peaks at *m/z* 353, 355, and 469 were detected in direct infusion mixture analysis that were absent in LC-ESI-MS/MS. The precursor peaks at *m/z* 353 and 355 are most likely hydroxylated metabolites of glyceollins, wherein the latter contains an additional reduced double

bond. The improved detectability in direct infusion ESI-MS/MS may be rationalized if one considers the additional acquisition time afforded by direct infusion that serves to improve signal-to-noise (S/N) ratios. Moreover, in LC-MS/MS experiments, the (S/N) ratios may not be maximized if spectra are averaged across the entire width of the chromatographic peak (due to weaker signals away from the center of the peak).[43] A literature example reports a 20-fold gain in sensitivity observed with direct infusion of LC fractions using multichannel acquisition, as compared to LC/MS.[44] Therefore, we suspect that the conditions employed for LC-ESI-MS/MS resulted in a detection limit just above the threshold for observation of these *m/z* 353, 355, and 469 signals.

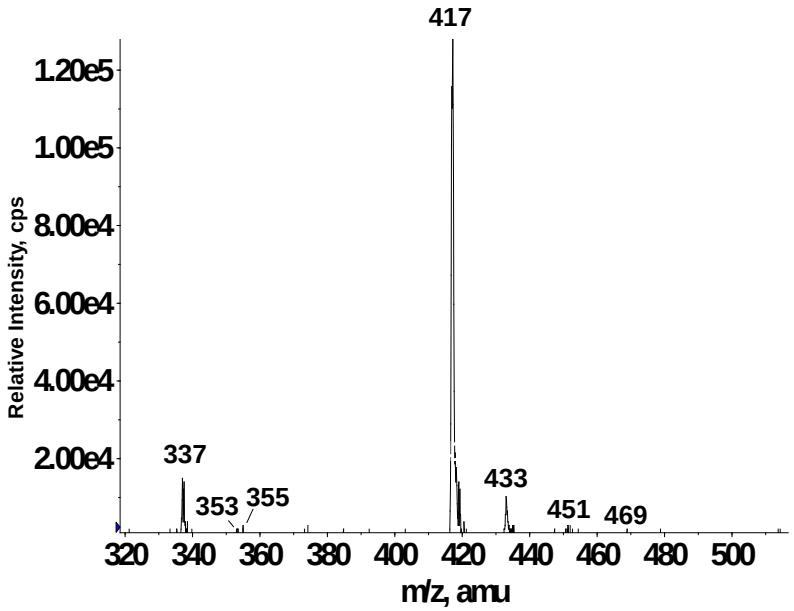

Figure 1-7: Direct infusion negative ion electrospray -75 V CID precursor ion scan of *m/z* 148 from rat plasma derived from rats.

1.5 Conclusion

A precursor ion scan method based on *m/z* 148 product ion formation was developed and optimized to screen for glyceollins and glyceollin related compounds, including metabolites. LC-ESI-MS/MS analyses with both precursor ion and product ion scans were carried out on a triple quadrupole to identify glyceollins and their metabolites in rat plasma. Precursor ion scanning of *m/z* 148 allowed the characterization of glyceollins' metabolites at *m/z* 417, 433, 353, and 355. After inspection and interpretation of obtained tandem mass spectra, accurate mass measurements of *m/z* 417 and 433 were performed, thus, confirming the *in vivo* sulfation, and sulfation plus oxygen addition, respectively, of glyceollins in rats. In addition, metabolites at *m/z* 353 and 355 were observed and were proposed to represent hydroxylated forms of glyceollins wherein the latter has one less double bond. Along with developing a method to screen for glyceollins and its related compounds, this study is the first to establish hydroxylation and sulfation metabolic pathways of glyceollins in dosed animals.

1.6 Acknowledgment

We thank Dr. Mark L. Heiman of NuMe Health for his expertise and input in designing the rat study, including identification of the vehicle. We thank Mr. Xiaohua Liu for performing accurate mass analyses by FT-ICR-MS. Financial support for this research was provided by the National Science Foundation through CHE-1058764. Additional financial support was provided by the MetaboHub project, by the Louisiana Cancer Research Consortium, and by NIH-RCMI grant #5G12RR026260 from the National Institute on Minority Health and Health Disparities. The contents are solely the responsibility of the authors and do not necessarily represent the official views of the Louisiana Cancer Research Consortium or the NIH.

1.7 References

1. Radhakrishnan, G.; Rashmi; Agarwal, N.; Vaid, N. B. *Internet Journal of Gynecology and Obstetrics.* 2009, 11(1), 12.

2. Oergaard, A.; Jensen, L. *Experimental Biology and Medicine*. 2008, 233(9), 1066-1080.

3. Miyanaga, N.; Akaza, H.; Hinotsu, S.; Fujioka, T.; Naito, S.; Namiki, M.; Takahashi, S.; Hirao, Y.; Horie, S.; Tsukamoto, T.; Mori, M.; Tsuji, H. *Cancer Science*. 2012, 103(1), 125-130.

4. Kingsley, K.; Truong, K.; Low, E.; Hill, C. K.; Chokshi, S. B.; Phipps, D.; West, A.; Keiserman, M. A.; Bergman, C. J. *Journal of Dietary Supplements.* 2011, 8(2), 169-188.

5. Sahin, K.; Tuzcu, M.; Sahin, N.; Akdemir, F.; Ozercan, I.; Bayraktar, S.; Kucuk, O. *Nutrition and Cancer.* 2011, 63(8), 1279-1286.

6. Merchant, K.; Kumi-Diaka, J.; Rathinavelu, A.; Esiobu, N.; Zoeller, R.; Hartmann, J.; Johnson, M. *Functional Foods in Health and Disease.* 2011, 1(3), 91-105.

7. Majid, S.; Kikuno, N.; Nelles, J.; Noonan, E.; Tanaka, Y.; Kawamoto, K.; Hirata, H.; Li, L. C.; Zhao, H.; Okino, S. T.; Place, R. F.; Pookot, D.; Dahiya, R. *Cancer Research.* 2008, 68(8), 2736-2744.

8. Barnes, S.; Sfakianos, J.; Coward, L.; Kirk, M. *Advances in Experimental Medicine and Biology*. 1996, 401(Dietary Phytochemicals in Cancer Prevention and Treatment), 87-100.

9. Boue, S. M.; Carter, C. H.; Ehrlich, K. C.; Cleveland, T. E. *Journal of Agricultural and Food Chemistry*. 2000, 48(6), 2167-2172.

10. Darvill, A. G.; Albersheim, P. *Annual Review of Plant Physiology*. 1984, 35, 243-75.

11. Tilghman, S. L.; Boue, S. M.; Burow, M. E. *Molecular and Cellular Pharmacology*. 2010, 2(4), 155-160.

12. Kim, H. J.; Suh, H.; Kim, J.; Park, S.; Joo, Y.; Kim, J.. *Journal of Agricultural and Food Chemistry.* 2010, 58(22), 11633-11638.

13. Park, S.; Ahn, I. S.; Kim, J. H.; Lee, M. R.; Kim, J. S.; Kim, H. J. *Journal of Agricultural and Food Chemistry.* 2010, 58(3), 1551-1557.

14. Rhodes, L. V.; Tilghman, S. L.; Boue, S. M.; Wang, S.; Khalili, H.; Muir, S. E.; Bratton, M. R.; Zhang, Q.; Wang, G.; Burow, M. E.; Collins-Burrow, Bridgette M. *Oncology Letters.* 2012, 3(1), 163-171.

15. Burow, M. E.; Boue, S. M.; Collins-Burow, B. M.; Melnik, L. I.; Duong, B. N.; Carter-Wientjes, C. H.; Li, Shuanfang; W., Thomas E.; Cleveland, T. E.; McLachlan, J. A. *Journal of Clinical Endocrinology and Metabolism*. 2001, 86(4), 1750-1758.

16. Salvo, V. A.; Boue, S. M.; Fonseca, J. P.; Elliott, S.; Corbitt, C.; Collins-Burow, B. M.; Curiel, T. J.; Srivastav, S. K.; Shih, B. Y.; Carter-Wientjes, C.; Wood, C. E.; Erhardt, P. W.; Beckman, B. S.; McLachlan, J. A.; Cleveland, T. E.; Burow, M. E. *Clinical Cancer Research*. 2006, 12(23), 7159-7164.

17. Zimmermann, C.; Tilghman, S. L; Boue, S. M; Salvo, V. A; Elliott, S.; Williams, K. Y.; Skripnikova, E. V.; Ashe, H.; Payton-Stewart, F.; Vanhoy-Rhodes, L. Fonseca, J. P.; Corbitt, C.; Collins-Burow, B. M.; Howell, M. H.; Lacey, M.; Shih, B. Y.; Carter-Wientjes, C.; Cleveland, T. E.; McLachlan, J. A.; Wiese, T. E.; Beckman, B. S.; Burow, M. E. *Journal of pharmacology and experimental therapeutics.* 2010, 332(1), 35-45.

18. Payton-Stewart, F.; Khupse, R. S.; Boue, S. M.; Elliott, S.; Zimmermann, M. C.; Skripnikova, E. V.; Ashe, H.; Tilghman, S. L.; Beckman, B. S.; Cleveland, T. E.; McLachlan, J. A.; Bhatnagar, D.; Wiese, T. E.; Erhard, P.; Burow, M. E. *Steroids*. 2010, 75(12), 870-878.

19. Wood, C. E.; Clarkson, T. B.; Appt, S. E.; Franke, A. A.; Boue, S. M.; Burow, M. E.; McCoy, Thomas; Cline, J. Mark. *Nutrition and Cancer.* 2006, 56(1), 74-81.

20. Payton-Stewart, F.; Schoene, N. W.; Kim, Y. S.; Burow, M. E.; Cleveland, T. E.; Boue, S. M.; Wang, T. Y. *Molecular Carcinogenesis.* 2009, 48(9), 862-871.

21. Boue, S. M.; Isakova, I. A.; Burow, M. E.; Cao, H.; Bhatnagar, D.; Sarver, J. G.; Shinde, K. V.; Erhardt, P. W.; Heiman, M. L. *Journal of Agricultural and Food Chemistry.* 2012, 60(25), 6376-6382.

22. Park, S.; Kim, D. S.; Kim, J. H.; Kim, J. S.; Kim, H. J. *Nutrition*. 2012, 28(2), 204-211.

23. Kim, H. J.; Lim, J.; Kim, W.; Kim, J. *Proceedings of the Nutrition Society.* 2012, 71(1), 166-174.

24. Hedin, P. A.; Phillips, V. A. *Journal of Agricultural and Food Chemistry*. 1992, 40(4), 607-11.

25. Crow, F. W.; Tomer, K. B.; Looker, J.H.; Gross, M. L. *Analytical Biochemistry.* 1986, 155(2), 286-307.

26. Kiehne A.; Engelhardt, U. H. *Zeitschrift fur Lebensmittel-Untersuchung und – Forschung.* 1996, 202(1), 48-54.

27. Jia-Ping. L.; Heng, L.; Jin, S.; Han-Ming, S.; Nam, O. *Journal of chromatography B.* 2007, 848(2), 215-25.

28. Ma, Y. L.; Heuvel, H.V..; Claeys, M. *Rapid Communications in Mass Spectrometry.* 1999, 13(19), 1932-1942.

29. Simons, R.; Vincken, J.; Bohin, M. C.; Kuijpers, T. F. M.; Verbruggen, M. A.; Gruppen, H. *Rapid Communications in Mass Spectrometry.* 2011, 25(1), 55-65.

30. Liu, Y.; Hu, M.. *Drug Metabolism and Disposition.* 2002, 30(4), 370-377.

31. Quadri, S. S.; Stratford R. E.; Boué; S. M.; Cole, R. B. "A New Mass Spectrometric Approach for Screening of Glyceollins and Their Metabolites" Proceedings of the 60th ASMS Conference on Mass Spectrometry and Allied Topics, Vancouver, BC, May 22, 2012.

32. Karni, M.; Mandelbaum, A. *Journal of Mass Spectrometry*. 1980, 15(2), 53-64.

33. Bowen, R. D.; Clifford, P.; Gallagher, R. T. *European Mass Spectrometry.* 1996, 2(4/5), 233-246.

34. Chen, K.; Rannulu, N. S.; Cai, Y.; Lane, P.; Liebl, A. L.; Rees, B. B.; Corre, C.; Challis, G. L.; Cole, R. B. *Journal of the American Society for Mass Spectrometry*. 2008, 19(12), 1856-1866.

35. Cai, Y.; Mo, Z.; Rannulu, N. S.; Guan, B.; Kannupal, S.; Gibb, B. C.; Cole, R. B. *Journal of Mass Spectrometry*. 2010, 45(3), 235-240.

36. Wahrhaftig, A.L. In Gaseous ion Chemistry and MS, *Futrell, J.H. (ed.)*; Wiley: New York, 1986; pp. 7–24.

37. McLafferty, F. W.; Tureček, F. Interpretation of Mass Spectra, 4th ed; University Science Books: California, 1993; pp 115-134.

38. Li, Z; Xue, F.; Xu, L.; Peng, C.; Kuang, H.; Ding, T.; Xu, C.; Sheng, C.; Gong, Y.; Wang, L. Journal of Chromatographic Science (2011) 49(4) 338-343.

39. Bolling, B. W.; Court, M. H.; Blumberg, J. B.; Chen, C.Y. Oliver. *Journal of Nutritional Biochemistry*. 2010, 21(6), 498-503.

40. Zhu, W.; Xu, H.; Wang, S.; Hu, M. *AAPS Journal.* 2010, 12(4), 525-536.

41. Levitz, M; Kadner, S; Young, B. K.; *Steroids*. 1976, 27(2), 287-294.

42. Cech, N; Enke, C; In Electrospray and MALDI Mass Spectrometry; Cole, Richard B.; Wiley: New Jersey, 2010; pp 49-74.

43. Zhang, Z.; McElvain, J. S.; *Analytical Chemistry*. 1999, 71(1), 39-45.

44. Hopfgartner, G.; Varesio, E.; Tschaeppaet, V.; Grivet, C.; Bourgogne, E.; Leuthold, L. A.; *Journal of Mass Spectrometry*. 2004, 39(8), 845-855.

CHAPTER 2

IDENTIFICATION OF GLYCEOLLIN METABOLITES DERIVED FROM CONJUGATION WITH GLUTATHIONE AND GLUCURONIC ACID IN RATS BY ON-LINE LIQUID CHROMATOGRAPHY-ELECTROSPRAY IONIZATION TANDEM MASS SPECTROMETRY

Syeda S. Quadri, Robert E. Stratford, Stephen M. Bou**é**, and Richard B. Cole

2.1 Abstract

Glyceollin-related metabolites produced in rats following oral glyceollin administration were screened and identified by precursor and product ion scanning using liquid chromatography coupled on-line with electrospray ionization tandem mass spectrometry (LC-ESI-MS/MS). Precursor ion scanning in the negative ion (NI) mode was used to identify all glyceollin metabolites based on production of a diagnostic radical product ion (*m/z* 148) upon decomposition. Using this approach, precursor peaks of interest were found at *m/z* 474 and 531. Tandem mass spectra of these two peaks allowed us to characterize them as by-products of glutathione conjugation. The peak at *m/z* 474 was identified as the deprotonated cysteinyl conjugate of glyceollins with an addition of an oxygen, whereas m/z 531 was identified as the deprotonated cysteinylglyceine glyceollin conjugate plus an oxygen. These results were confirmed by positive ion (PI) mode analyses. Mercapturic acid conjugates of glyceollins were also identified in NI mode as deprotonated molecules at *m/z* 500. In addition, glucuronidation of glyceollins was observed, giving a peak at *m/z* 513 corresponding to the deprotonated conjugate. Production of glucuronic acid conjugates of glyceollins was confirmed *in vitro* in rat liver microsomes. Neither glutathione conjugation by-products nor glucuronic acid conjugates of glyceollins have been previously reported.

2.2 Introduction

Cancer is the second leading cause of death in the United States after heart disease,[1] yet there is still no cure for this disease. Soybean isoflavones have been shown to exhibit anti-cancer and anti-proliferative activity toward cancerous cells.[2,3] Much of the research concerning isoflavones has been conducted on diadzein and genistein.[4-8] Among the more recently studied isoflavones are the glyceollins that are also produced by soybeans under stressed conditions (e.g., UV light exposure or infection by *Aspergillus*).[9,10] Glyceollins, like other soy isoflavones, are non-steroid compounds that have diphenolic groups which closely resemble the steroid structure of estradiol.[11] Several propositions have been offered to explain the mechanism of inhibition of cancer by soy isoflavones through antiestogenic activity by interfering cancer cells' ability to respond to estradiol.[10,17]

Recent investigations have proposed glyceollins as prevention or therapy candidates for breast, ovarian, and prostate cancers.[12,17] Glyceollins exhibit anti-estrogenic effects on estrogen receptor function and estrogen-dependent tumor growth.[13,14] Breast cancer (MCF-7) and ovarian cancer (BG-1) cell proliferation, which is induced by estrogen, was found to be inhibited by glyceollins.[15] Furthermore, studies conducted on post-menopausal monkeys and human prostate cancer cell line (LNCaP) also showed a reduction in cancer progression by glyceollins.[16,17] The potential anticancer benefits of glyceollins have been well documented, but its metabolism is not well understood[18] other than the evidence for sulfation.[19]

Typically, drugs are eliminated or detoxified from the body through phase I and II metabolism.[20] Phase I results in oxidation, reduction, or hydrolysis of a drug.[21,22] Phase II conjugation is a common pathway for isoflavone metabolism which results in methylation,

sulfation, glucuronidation, and glutathione conjugation.[23,24,25] Some of the metabolic pathways that are involved in drug detoxification, in particular glutathione conjugation, have been shown to promote drug resistance and/or additional adverse health effects during cancer treatment.[26] Therefore, it is extremely important to have a thorough understanding of metabolic pathways. Metabolism of genistein has been well studied and it is known to undergo sulfation and glucuronidation,[27,28,29] but much less is known about glyceollins metabolism. A recent study conducted on rats reported absorption of glyceollins across the gastrointestinal tract of rats. Maximum plasma concentrations of 160 ng/ml were attained in rats within 4 hr of oral administration of a single dose of 90 mg/kg.[30] The current *in vivo* study builds upon our previous identifications of sulfated metabolites of glyceollins found in rat plasma[19] by investigating glyceollin metabolites in rat plasma and feces.

2.3 Experimental Method

2.3.1 Extraction of glyceollin isomers

Using a procedure developed at the Southern Regional Research Center (ARS, USDA, New Orleans, LA), a mixture of glyceollins I, II, and III was obtained. Briefly, after slicing, soybean seeds (1 kg) were inoculated with *Aspergillus sojae*. Three days later, the glyceollins were extracted from the inoculated seeds with 1 L methanol (Aldrich Chemical Co., St. Louis, MO). The glyceollins were isolated using preparative scale HPLC employing two Waters (Milford, MA) 25 x 100 mm, 10 µm particle size µBondapak C_{18} radial compression column segments; the column segments were combined using an extension tube. HPLC was performed on a Waters 600E equipped with a Waters UV-Vis 996 detector scanning from 210-400 nm. The injection volume was 20 mL; the flow rate was 8.0 mL/min using the following solvent gradient: A = acetonitrile (Aldrich Chemical Co.), B = water (Millipore system, Billerica, MA) 5% A for 10 min, then 5% A to 90% A in 60 min followed by holding at 90% A for 20 min. The fraction containing the glyceollins was concentrated under vacuum and freeze-dried. Confirmation of individual glyceollins was based on HPLC retention time and UV-Vis absorbance spectra comparison with those of authentic standards isolated at SRRC. UV-Vis spectrophotometry at 285 nm was used to estimate the percentage of the three isomers used in all experiments: glyceollin I (68%), glyceollin II (21%), and glyceollin III (11%).

2.3.2 *Glyceollin dosing of rats and plasma sample collection*

The procedures used for administration of glyceollins to rats and subsequent sample collection have been previously described.[31] Briefly, glyceollins dissolved in poloxamer were administered (90 mg/kg) via oral gavage (3 mL) to male ZDSD rats (PreClinOmics, Indianapolis, IN) that were subjected to a 12:12 hr light-dark cycle. Rats (approx. 500 g wt.) were euthanized

at various time points by decapitation; trunk blood was subsequently collected into EDTA-coated tubes supplemented with aprotinin. Plasma was separated and stored at -80 ^{o}C. Upon thawing, 125 µL of plasma was transferred into microcentrifuge tubes to which an equivalent volume of acetonitrile was added. The mixture was vortexed, then centrifuged at 10,000 rpm for 20 min. The supernatant was subjected to mass spectrometric analysis.

2.3.3 *Urine sample treatment*

A urine sample obtained from a 24 hr collection period that commenced following a single 90 mg/kg oral dose to a rat was acidified with 1% TFA, vortexed, and centrifuged at 10,000 rpm for 10 min. The supernatant was diluted with 1:1 0.2% formic acid in 10% acetonitrile and stored at -80 ^{o}C until ready for LC-MS analyses.

2.3.4 *Fecal sample collection*

Feces from rats were collected prior to, and after the dosage of glyceollins (90 mg/kg). In the latter case, samples were obtained following 2-weeks of once-daily dosing. Both the pre- and post-dosed fecal pellets were weighed and a 1:2 (pellet weight: vol) ratio of deionized water was added to each group. A smooth paste was created in a glass mortar and pestle. The paste was then transferred to a polypropylene tube and diluted with CH_3CN 1:2 (paste wt: vol). The tubes were centrifuged for 5 min at 1000 rpm. Supernatant was collected and transferred to fresh tubes; then approximately 0.1 g of ammonium acetate was added progressively with gentle vortexing. Tubes were subsequently centrifuged for 5 min at 1000 rpm. The supernatant (acetonitrile layer) was collected and stored at -70 ^{o}C until analysis.

2.3.5 *Liver Microsomes treatment with UDPGA cofactor*

Samples were prepared in triplicate for both the control and the experimental group. 134 µL of KH_2PO_4 buffer, 20 µL of 20 mg/mL rat liver microsomes, and 4 µL of 5 mg/mL alamethicin

was added to 1.5 mL eppendorf tubes, vortexed, and incubated for 15 min. 20 µL of $MgCl_2$ and 2 µL of 1 mM substrate were then added, vortexed and incubated for 3 min. 20 µL of KH_2PO_4 buffer and 20 µL of 10 mM UDPGA were added to control and experimental groups, respectively. The tubes were incubated for 60 min at 37 ^oC. 200 µL of cold acetonitrile was added to each tube to terminate the incubation. Tubes were then vortexed followed by centrifugation for 5 min at 4000 rpm. Supernatant was transferred to fresh tubes and stored at -70 ^oC until analysis.

2.3.6 *Liquid Chromatography-Mass Spectrometry*

LC-ESI-MS and LC-ESI-MS/MS analyses were conducted on an Agilent 1200 series LC system (Agilent, Santa Clara, CA) coupled to a 3200 QTrap triple quadrupole mass spectrometer (Applied Biosystems/MDS SCIEX, Foster, City, CA). Separation was performed on an Agilent Eclipse - XDB C18 column (4.6 x 150 mm ID, 5 µm). 10 µL was injected onto the column held at 25 ^oC. The binary mobile phase consisted of mobile phase A (water with 0.1% formic acid) and mobile phase B (acetonitrile with 0.1% formic acid). The gradient was 0-104 min 5% B to 100% B. Flow rate was 0.500 mL/min. The UV absorbance detector was set at 285 nm.

For negative ion LC-ESI-MS and LC-ESI-MS/MS analyses, electrospray parameters were set at: curtain gas (CUR) 20 psi, ionspray voltage (IS) -4500 V, GAS1 60 psi, GAS2 60 psi, source temperature 600 ^oC, CAD gas pressure 6 psi, entrance potential (EP) -10 V, collision cell exit potential (CXP) -3 V. Declustering potential (DP) and collision energy (CE) were optimized to be -55 V and -34 eV, respectively. For positive ion experiments, CUR, IS, EP, CXP, DP and CE were maintained at 10 psi, 5000 V, 10 V, 5 V, 40 V, and 30 eV, respectively. All other parameters were the same as for negative ion mode. The information-dependent

acquisition (IDA) method was employed to perform full scan and precursor ion scans sequentially (scan rate = 1 sec/200 Da). Tandem spectrometry was then carried out on precursors of interest.

2.4 Results and Discussion

2.4.1 Precursor ion scans of m/z 148

In our previous work, we proposed a precursor ion scan method to screen for isomeric glyceollins and their metabolites based on a diagnostic radical product ion.[19,32] The high energy CID product ion spectrum of glyceollins yields an exceptionally stable radical at *m/z* 148, which serves as a "signature" common to all three glyceollins isomers.[19] Employing this negative ion developed methodology based upon scanning for precursors of *m/z* 148, plasma and feces samples from rats dosed with isomeric glyceollins I, II, and III were screened for the glyceollins and their metabolites by LC-ESI-MS and LC-ESI-MS/MS. The precursor ion scanning of *m/z* 148 for rat feces samples resulted in the appearance of many more metabolites compared to rat plasma samples. Figure 2-1 shows a representative LC chromatogram of a rat feces sample. All three unmetabolized isomers of glyceollins (*m/z* 337) were detected. Peaks labeled 9, 8 and 10 on the LC chromatogram correspond to glyceollin I, II, and III, respectively.

Little is known about glyceollins metabolism, but our findings from rat feces indicate that extensive oxidation of glyceollins has occurred. Peaks 5, 1, and 6 represent m/z 148 precursors at *m/z* 353, 371, and 387, respectively. Relative to deprotonated glyceollins (m/z 337), these three metabolites are proposed as products of epoxidation and/or OH/H replacment of glycoleollins (*m/z* 353); diol addition at a double bond (*m/z* 371), , and a combination of the two processes above, i.e., diol addition at a double bond plus epoxidation and/or OH/H replacment (m/ 387). Two of the three above-mentioned peaks observed in rat feces (m/z 371, 387) were also detected in rat urine, as was m/z 451 (the latter likely represents glyceollins that are both hydrolyzed and sulfated). The above peaks were only observed in rat feces. LC-ESI-MS/MS precursor ion scanning of *m/z* 148 from rat feces showed additional peaks eluting at 14.4, 16.8, 19.3, 30.9, and 35.3 min. These

chromatographic peaks correspond to glyceollins metabolite precursors at *m/z* 531, 474, 433, 417, along with deprotonated glyceollins at m/z 337, respectively. These latter five precursors of m/z 148 were also found in *rat plasma*, whereas m/z 531 and 474 were observed from rat urine (data not shown). Sulfation and sulfation plus an oxygen of glyceollins account for the peaks observed at *m/z* 417 (peak 7) and 433 (peak 4), respectively, as discussed previously.[19] Two remaining precursor peaks of interest appear at *m/z* 474 and 531. These were considered as phase II metabolites of glyceollins and were further investigated by tandem mass spectrometry as discussed in the following section.

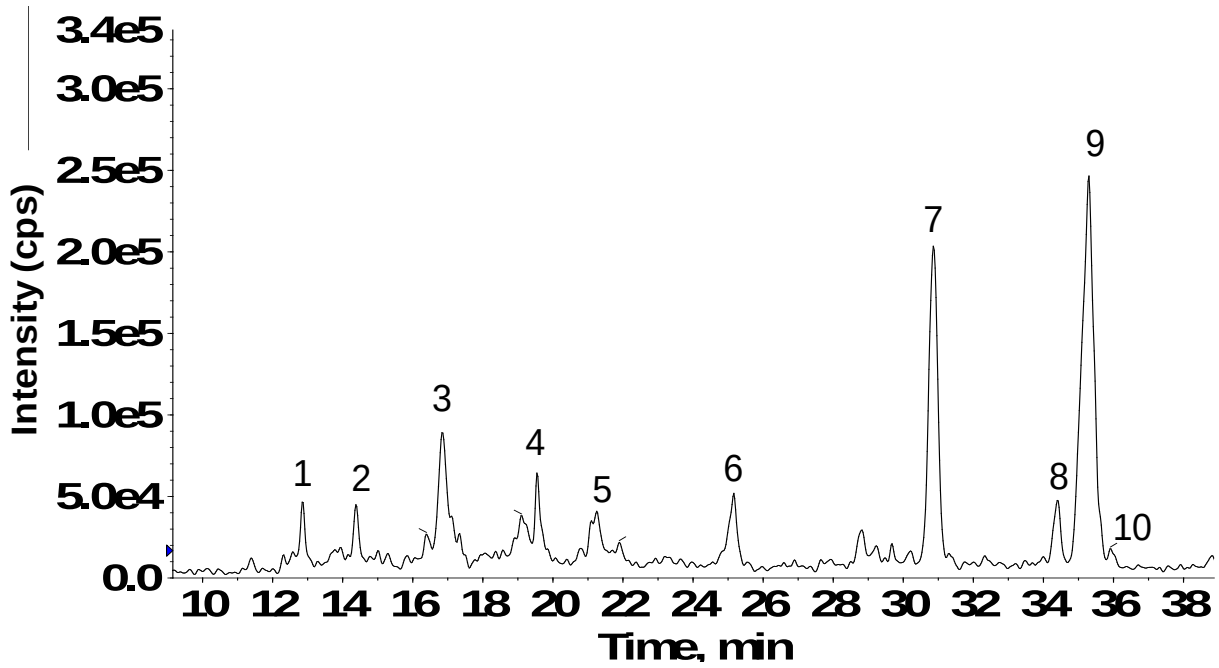

Figure 2-1: LC-ESI-MS/MS precursor ion scans showing total ion current of all precursors of *m/z* 148 from feces of rats dosed orally once-daily for two weeks with 90 mg/kg of the glyceollin isomeric mixture.

2.4.2 Identification of Glyceollins' metabolites by LC-ESI-MS and LC-ESI-MS/MS

A chromatographic peak corresponding to the m/z 531 precursor from feces samples eluted at 14.4 min (Figure 2-1) and an identical peak was also observed from rat plasma. The NI mode LC-ESI-MS/MS CID product ion mass spectrum of this *m/z* 531 precursor (Figure 2-2a) from feces summed across the entire chromatographic peak showed a fragment at *m/z* 353, which corresponds to a loss of 178 Da. Appearing in Figure 2-2b is the NI mode LC-ESI-MS/MS CID product ion mass spectrum of *m/z* 474 corresponding to a chromatographic peak eluting at 17.0 min (Figure 2-1). Similar to the result shown in Figure 2-2a, the m/z 474 also yields a fragment at *m/z* 353, indicating this time, a loss of 121 Da. The combined information extracted from Figures 2.2a and 2.2b point to the deduction that glutathione conjugation has occurred to glyceollins and that subsequent metabolic by-products of glutathione breakdown are present in both the rat feces and plasma samples. We propose that the loss of 178 Da (Fig. 2.2a) corresponds to departure of intact cysteinylglycine from the m/z 531 precursor that corresponds to a cysteinylglyceine conjugate of an oxygenated form of glyceollins. Strongly supporting this proposition is the appearance of a cysteinyl-glycine fragment ion at m/z 143 (Fig. 2.2a). To complement this information, the 121 Da loss from the m/z 474 precursor (Fig. 2.2b) is proposed to correspond to intact cysteine loss from the cysteinyl conjugate of oxygenated glyceollins. Further evidence to support this assignment is given by the appearance of m/z 387 that corresponds to decomposition of the cysteine amino acid (Fig. 2.2b).

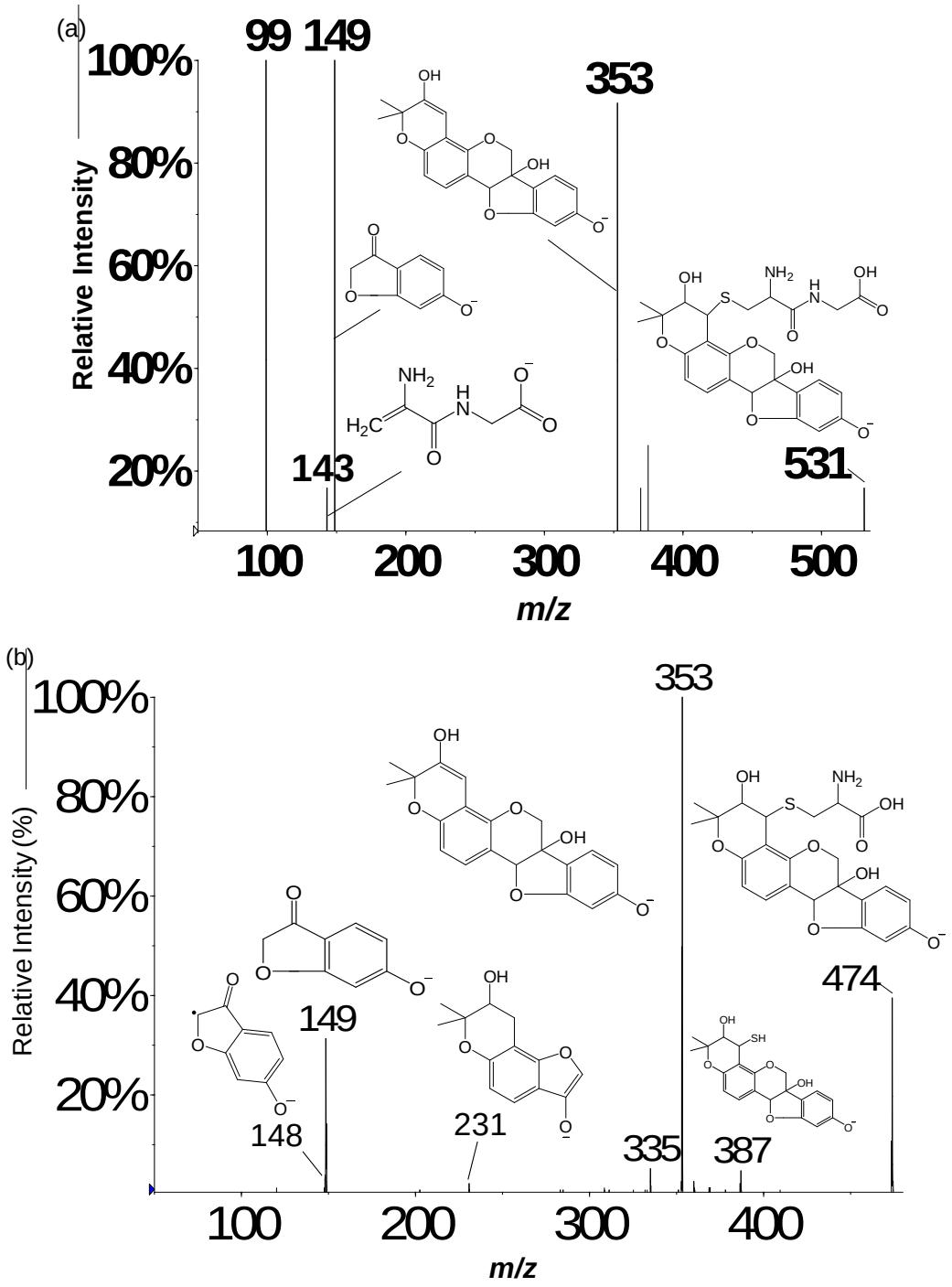

Figure 2-2: LC-ESI-MS/MS product ion spectrum of: (a) *m/z* 531 precursor and (b) *m/z* 474 precursor in negative ion mode. One site of hydroxylation and one site of peptide addition is shown; Scheme 1 shows other possible isomeric structures.

To further support these structural assignments, we consider that isoflavones are generally biotransformed into metabolites with increased water solubility compared to the original forms in order to facilitate excretion from the body. The major pathway through which these isoflavones are converted into metabolites is through phase II metabolism. Among the various detoxification mechanisms of drugs, the glutathione (GSH) metabolic pathway plays a major role in phase II detoxification.[34] GSH, consisting of glutamine (glu), cysteine (cys), and glycine (gly) amino amino acids.[33,34] forms conjugates with drugs and other xenobiotics with the assistance from Glutathione *S*-transferases (GSTs).[35] The first step of GSH breakdown, even when conjugated, involves hydrolysis of the γ-glutamyl bond by γ-glutamyltranspeptidase to form glutamic acid and (conjugated) cysteinylglycine; the cysteinylglycine can be further broken down into glycine and (conjugated) cysteine.[36,37] The cysteine conjugates can then be further metabolized via acetylation of the N-terminal amine of cysteine to form mercapturic acid conjugates.[38]

The glyceollin metabolites detected in rat plasma, urine and feces appear to have undergone glutathione conjugation. Although NI mode LC-ESI-MS/MS CID product ion mass spectra of potential *m/z* 660 and 644 precursors (corresponding to oxygenated and non-oxygenated GSH-glyceollins, respectively) were acquired from rat plasma, urine, and feces samples, no intact glutathione conjugates of glyceollins were found. This can be attributed to the fast kinetics of enzymatic glutamine cleavage from GSH-glyceollins complex that results in cysteinylglyceine conjugates of glyceollins (m/z 531, Figure 2-2a). As mentioned above, cysteinylglyceine conjugates are subsequently broken down into cysteine conjugates. The product ion spectrum of the m/z 474 precursor (Figure 2-2b) corroborates the presence of cysteinyl conjugates of glyceollins. These proposed metabolites are observed in oxygenated forms, i.e., in addition to the cysteinyl sulfur linkage, an oxygen atom has been added. We propose that the addition of oxygen

(Phase I metabolism) facilitates the subsequent addition of GSH (Phase II metabolism). Enzymatic formation of epoxides followed by glutathione conjugation has been well documented.[39,40] Epoxide formation at a double bond leads to a reactive intermediate that is highly susceptible to GSH complex formation. There are four possible 1,2-addition products (Scheme 2.1).

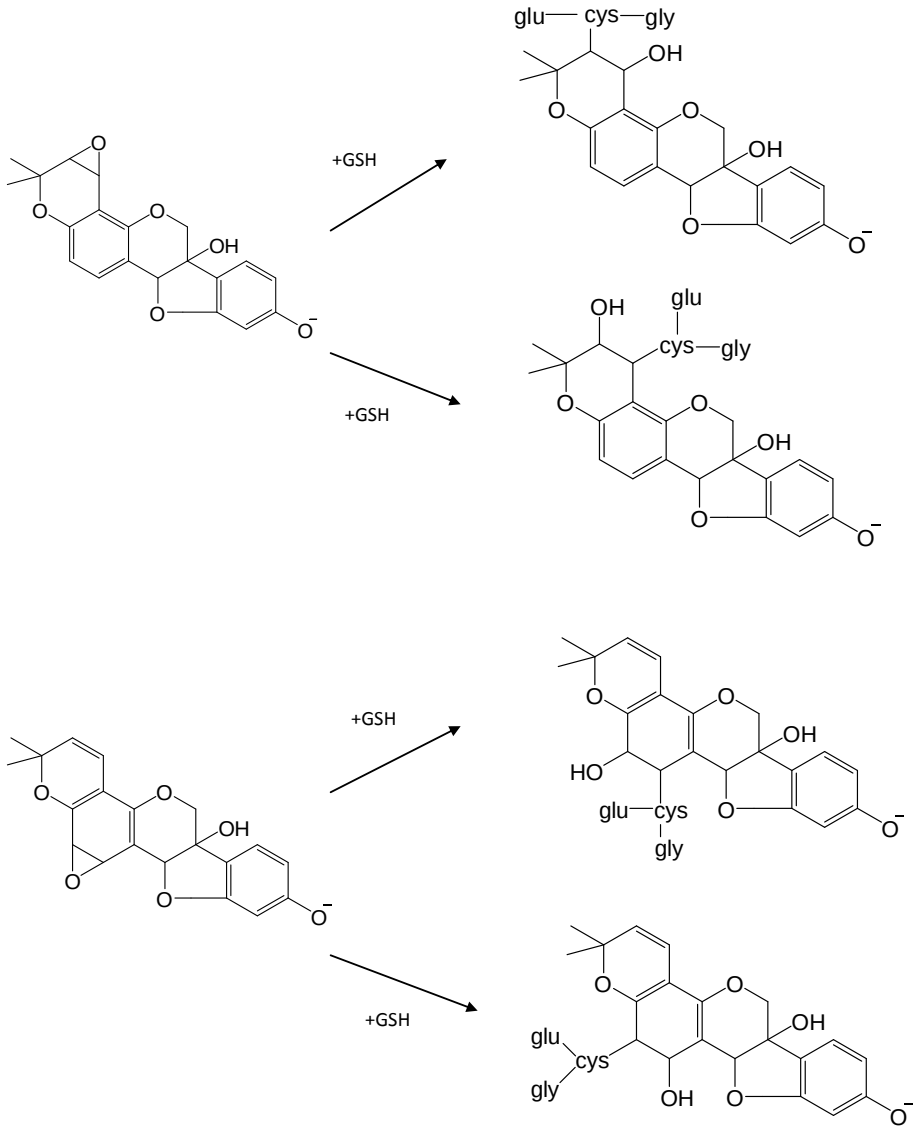

Scheme 2.1: Glutathione conjugation to two most favorable epoxide forms of glyceollin I.

The CID product ion mass spectra of m/z 531 (Figure 2-2a) and 474 (Figure 2-2b) each yield a fragment at m/z 353 corresponding to the loss of cysteinylglycine or cysteine, respectively, with abstraction of a neighboring hydrogen and double bond (or epoxide) formation on the glyceollins in each case. In addition, Figures 2.2a and 2.2b each show the presence of *m/z* 149, i.e., the B fragment ion formed from decomposition of the glyceollin backbone.[19] In our previous study, the CID product ion spectrum of the sulfated metabolite of glyceollins with an additional oxygen (m/z 433) showed B fragments (m/z 148, and 149) were the same as those found for unmetabolized deprotonated glyceollins, whereas A fragments (m/z 191 and 243) were shifted higher by 16 mass units. These combined observations allowed the localization of oxygen attachment on glyceollins.[19] For the GSH breakdown products, the appearance of the m/z 149 fragment suggests that the oxygen and cysteinylglyceine dipeptide or cysteine are not located on the B fragments. More importantly, the A fragment expected at m/z 215[7,19] has been shifted to m/z 231 (Figure 2-2b), thus indicating that oxygen addition had occurred on the A fragment. Structures of oxygenated cysteinylglyceine- and cysteinyl- glyceollin conjugates are proposed in Figure 2-2a and 2.2b, respectively. Based upon our evidence for initial epoxidation followed by GSH attachment, combined with the CID data presented above, we conclude that there are only four possible structures for the oxygenated cysteinylglyceine- and cysteinyl- glyceollin conjugates (Scheme 2.2). These assignments of oxygenated cysteinylglyceine (m/z 531 in NI mode) and oxygenated cysteinyl (m/z 474 in NI mode) glyceollin conjugates were further confirmed by acquiring data in positive ion mode. Figure 2-3a and 2-3b show the PI mode LC-ESI-MS/MS CID product ion mass spectra of *m/z* 533 (protonated cysteinylglyceine glyceollins with an additional oxygen) and m/z 476 (protonated cysteinyl glyceollins with an additional oxygen). The appearance of m/z 355 corresponds to the loss of 178 Da from m/z 533 (Figure 2-3a) and 121 Da from m/z 476 (Figure

2-3b), indicating a loss of intact cysteinylglyceine or cysteine, respectively, that mirror the losses observed in the NI mode.

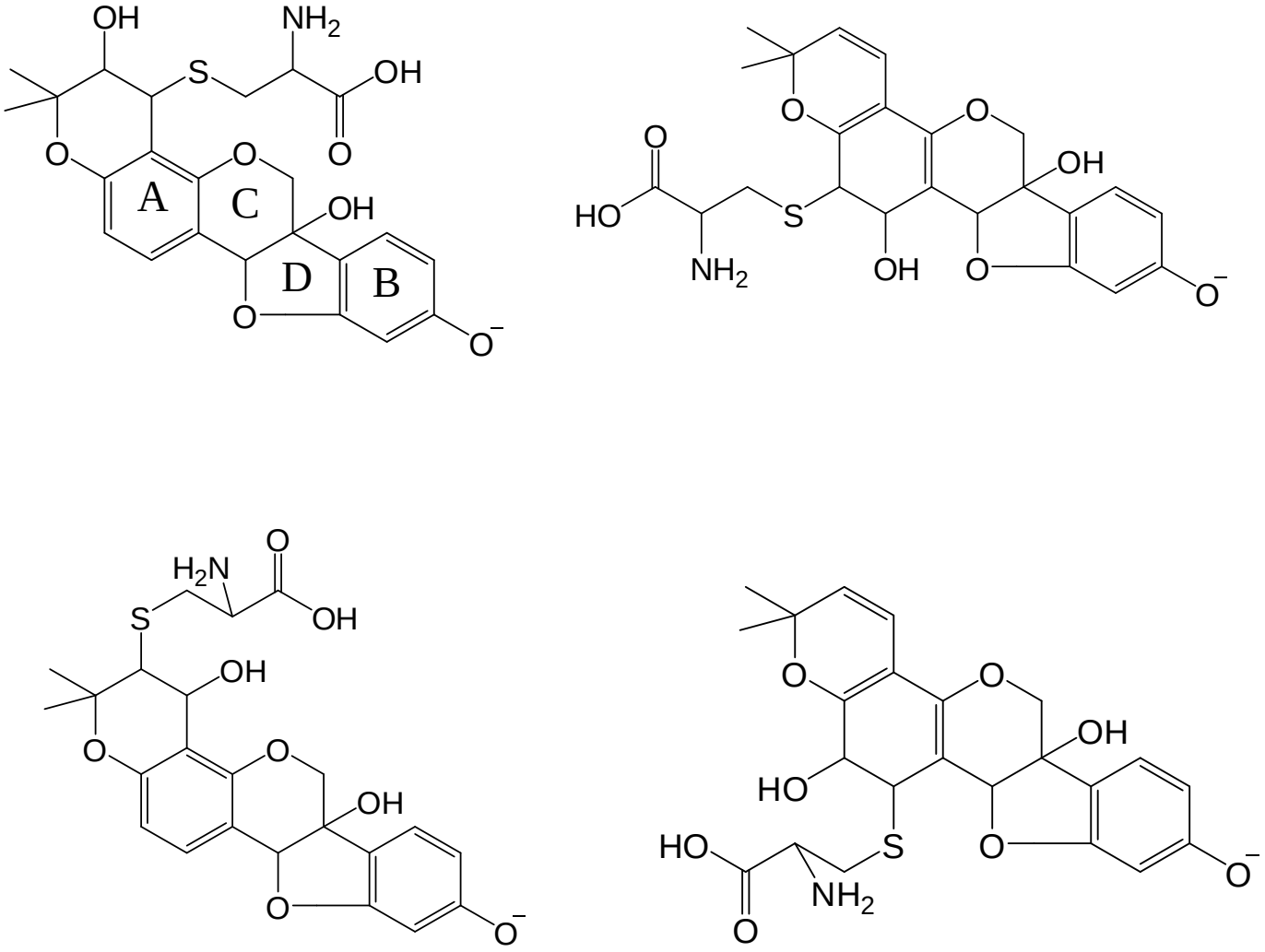

Scheme 2.2: Isomeric structures of oxygenated cysteinyl glyceollin I.

Cysteine conjugates can be further metabolized and acetylated, resulting in mercapturic acid conjugates as mentioned above. However, these anticipated conjugates were not detected in the precursor ion scan of *m/z* 148. Consequently, screening for mercapturic acid conjugates of glyceollins was directly performed by product ion scanning. The NI mode LC-ESI-MS/MS CID product ion mass spectrum of m/z 516 (corresponding to the previously detected m/z 474 cysteinyl glyceollins with additional oxygen peak that had potentially undergone acetylation) was performed on rat plasma, urine, and feces samples. Only feces eluted a chromatographic peak corresponding to m/z 516 that appeared at 22.9 min. The NI mode LC-ESI-MS/MS CID product ion mass spectrum of the *m/z* 516 precursor showed a fragment at *m/z* 353 corresponding to the loss of mercapturic acid (163 Da) from the oxygenated mercapturic acid conjugates of glyceollins. Other fragments similar to those in the CID product ion spectrum of deprotonated glyceollins were detected at m/z 148, 149, and 161; however, the signal for m/z 148 was very low.

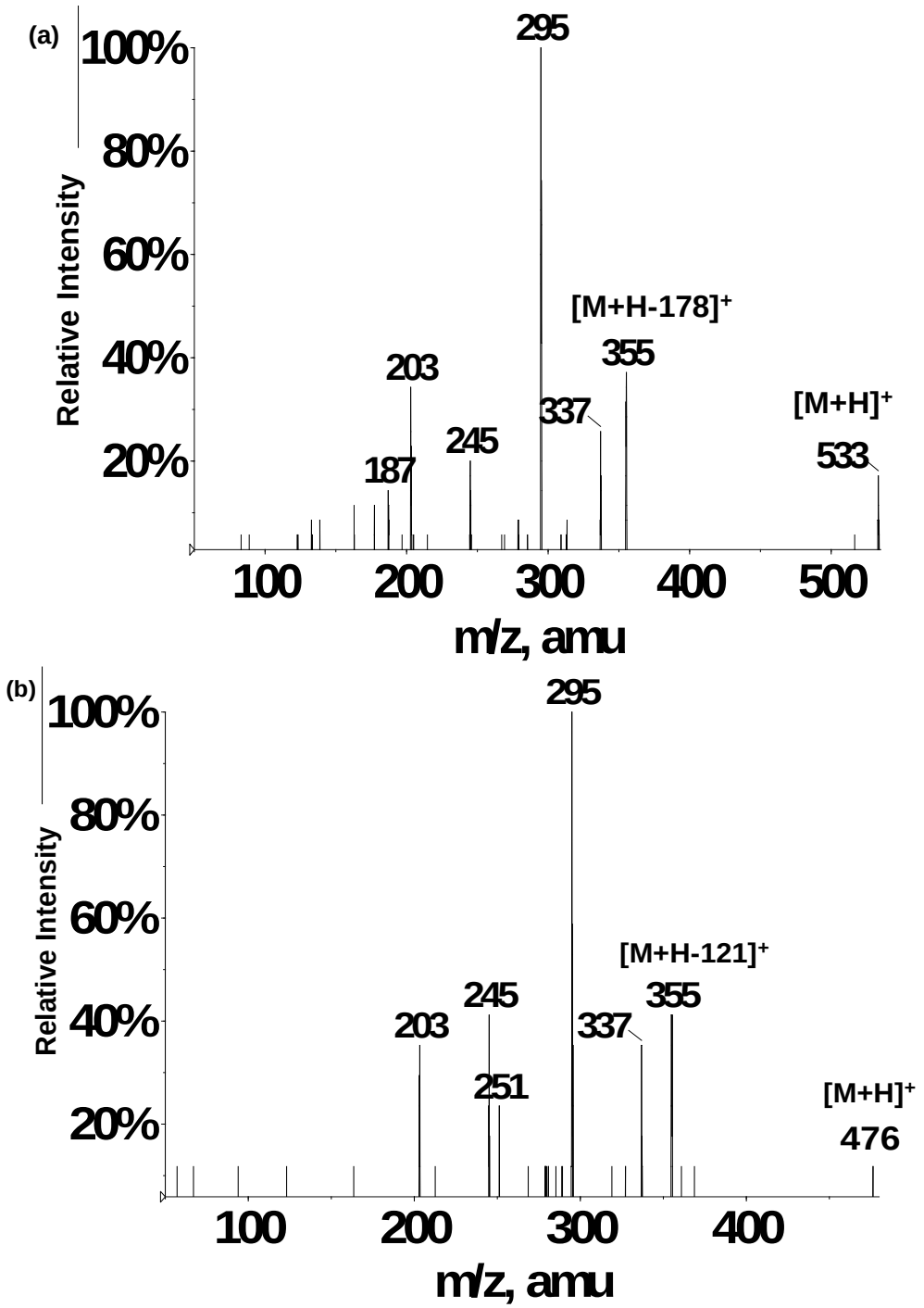

Figure 2-3: LC-ESI-MS/MS product ion spectra of (a) *m/z* 533 precursor and (b) *m/z* 476 precursor in positive ion mode.

2.4.3 Glucuronidation of glyceollins

Because glucuronide conjugates have been reported for isoflavones,[41,42,43] the decision was made to screen for glucuronide conjugates of glyceollins by performing product ion scans. In general, an addition of 176 Da in biological medium is well documented to be characteristic of addition of glucuronic acid.[28,44] Thus, the LC-ESI-MS/MS CID product ion scan of *m/z* 513 was carried out on rat plasma, urine, and feces samples, but a corresponding chromatographic peak appeared at 27.6 min from rat plasma and urine samples only. The averaged product ion mass spectrum (Figure 2-4) shows a peak at m/z 337 corresponding to deprotonated glyceollins production after loss of glucuronic acid. In addition, the highest abundance fragment appears at *m/z* 175. Even though a low abundance product ion at m/z 175 had been observed during CID of deprotonated glyceollins (*m/z* 337),[7,19] the high abundance of m/z 175 in Fig. 5 is better rationalized as release of glucuronate anion. No fragment ions in Figure 2-4 are shifted by 176 mass units relative to the product ions in the CID spectrum of m/z 337 (deprotonated glyceollins), indicating that the glucuronide moiety is the most labile substitutent of the m/z 513 precursor. Other CID product ions are assigned as consecutive decompositions of m/z 337, including m/z 319 (water loss) and *m/z* 149 production, but *m/z* 148 is absent. This latter product ion is not always observed upon *consecutive* decompositions as it requires relatively high energy CID conditions.[19] That is, owing to the energy consumed in decomposing *m/z* 513 to *m/z* 337, less energy remains for *m/z* 337 to undergo consecutive decomposition, which results in more favorable kinetics for *m/z* 149 production relative to *m/z* 148. This also rationalizes the absence of *m/z* 513 in the scan for precursors of *m/z* 148 spectrum.

Glucuronide conjugates of glyceollins for LC-ESI-MS/MS method development are not commercially available. Nonetheless, *in vitro* glucuronidation is often performed with the aid of

uridine diphosphoglucuronosyl-transferase enzymes (UGTs).[45] The UGT enzymes are present in abundance in rat liver microsomes. Using this approach, rat liver microsomes were treated with glyceollins to generate glucuronide conjugates of glyceollins. LC-ESI-MS/MS analyses were then carried out. The retention time and the similar fragmentation pattern in product ion spectrum of *m/z* 513 (Figure 2-4b) confirmed our assignment of glucuronidated metabolite of glyceollins from rat plasma and urine samples.

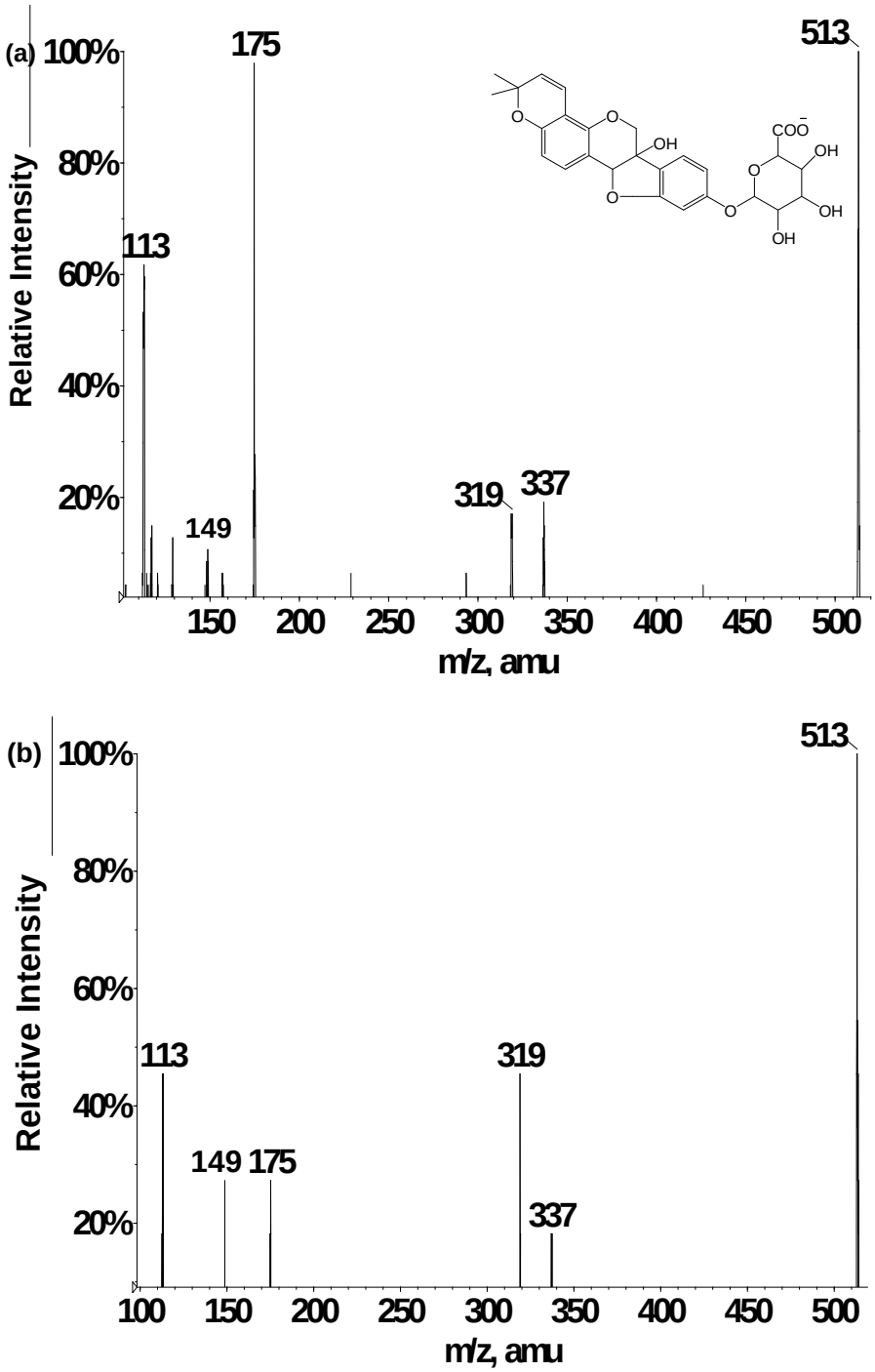

Figure 2-4: LC-ESI-MS/MS product ion spectrum of *m/z* 513 precursor corresponding to glucuronic acid conjugates of glyceollins acquired from (a) rat urine and (b) rat liver microsomes.

2.5 Conclusion

LC-ESI-MS/MS analyses were carried out on a triple quadrupole to identify glyceollins and their metabolites from rat plasma, urine, and feces. The precursor ion scan of *m/z* 148 allowed screening for glyceollin-related compounds. Peaks of interest were found at *m/z* 474 and 531 in rat plasma, urine, and feces samples, which were further investigated by product ion scanning. Tandem mass spectra of *m/z* 474 and 531 acquired in negative ion mode provided evidence for the glutathione conjugation pathway. The *m/z* 474 and 531 were identified as cysteine and cysteinylglyceine conjugates of glyceollins with an addition of an oxygen, respectively. The assignments were further confirmed by examining these conjugates in positive ion mode. We proposed that the formation of these Phase II metabolites is facilitated by epoxide formation (Phase I metabolism) on glyceollins. Four possible isomeric structures are proposed based upon tandem mass spectrometry fragmentation patterns. Oxygenated forms of mercapturic acid conjugates of glyceollins (m/z 516) were found to be present in rat feces, but not in rat plasma or urine. On the other hand, glucuronide conjugates of glyceollins were detected in rat plasma and urine. The identification of glucuronide conjugates of glyceollins was confirmed by *in vitro* glucuronidation of glyceollins by rat liver microsomes. To our knowledge, this is the first study to establish glutathione and glucuronide pathways of glyceollin metabolism. Oxygenated and non-oxygentated forms of cysteinylglycine, cysteine and mercapturic acid conjugates of glyceollins are reported along with glucuronide conjugates of glyceollins from glyceollin-dosed animals.

The scan for precursors of *m/z* 148 is thus a powerful method which allowed the characterization of glyceollin metabolites which may otherwise be difficult to pin-point, such as the newly reported oxygenated GSH by-product conjugates found here. These GSH by-product conjugates yielded mostly neutral losses of the peptide portion during tandem mass spectrometry.

Thus, these conjugates may have been overlooked if they were screened for by use of conventional product ion scans that rely on the appearance of charged peptide fragments. Because the appearance of m/z 148 in precursor ion scans requires optimized CID energies, which may vary according to the particular metabolite, the only caveat to this method is that all metabolites may not be detected using a single experimental condition (as was the case of mercapturic acid and glucuronide conjugates in this study).

2.6 References

1. Hoyert, D.; Xu, J.; *National Vital Statistics Reports*. 2012, 61(6), 1-52.

2. Xu, X.; Duncan, A. M.; Merz, B. E.; Kurzer, M. S. *Cancer Epidemiology, Biomarkers & Prevention*. 1998, 7(12), 1101-1108.

3. Miyanaga, N.; Akaza, H.; Hinotsu, S.; Fujioka, T.; Naito, S.; Namiki, M.; Takahashi, S.; Hirao, Y.; Horie, S.; Tsukamoto, T.; Mori, M.; Tsuji, H. *Cancer Science*. 2012, 103(1), 125-130.

4. Barnes, S.; Prasain, J.; D'Alessandro, T.; Arabshahi, A.; Botting, N.; Lila, Mary A.; Jackson, G.; Janle, E. M.; Weaver, C. M. *Food & Function* . 2011, 2(5), 235-244.

5. Barnes, S.; Sfakianos, J.; Coward, L.; Kirk, M. *Advances in Experimental Medicine and Biology*. 1996, 401(Dietary Phytochemicals in Cancer Prevention and Treatment), 87-100.

6. Majid, S.; Kikuno, N.; Nelles, J.; Noonan, E.; Tanaka, Y.; Kawamoto, K.; Hirata, H.; Li, L. C.; Zhao, H.; Okino, S. T.; Place, R. F.; Pookot, D.; Dahiya, R. *Cancer Research.* 2008, 68(8), 2736-2744.

7. Simons, R.; Vincken, J.; Bohin, M. C.; Kuijpers, T. F. M.; Verbruggen, M. A.; Gruppen, H. *Rapid Communications in Mass Spectrometry.* 2011, 25(1), 55-65.

8. Qi, W.; Weber, C. R.; Wasland, K.; Savkovic, S. D. *BMC Cancer* . 2011, 11, 219.

9. Boue, S. M.; Carter, C. H.; Ehrlich, K. C.; Cleveland, T. E. J. *Agric. Food Chem*. 2000, 48 (6), 2167−2172.

10. Burow, M. E.; Boue, S. M.; Collins-Burow, B. M.; Melnik, L. I.; Duong, B. N.; Carter-Wientjes, C. H.; Li, Shuanfang; W., Thomas E.; Cleveland, T. E.; McLachlan, J. A. *Journal of Clinical Endocrinology and Metabolism*. 2001, 86(4), 1750-1758.

11. Setchell KDR, Adlercreutz H. Mammalian lignans and phyto-oestrogens. Recent Studies on their formation, metabolism and biological role in health and disease. In: Rowland IA, ed. The Role of Gut Microflora in Toxicity and Cancer. New York: Academic Press 1988:315-345.

12. Rhodes, L. V.; Tilghman, S. L.; Boue, S. M.; Wang, S.; Khalili, H.; Muir, S. E.; Bratton, M. R.; Zhang, Q.; Wang, G.; Burow, M. E.; Collins-Burrow, Bridgette M. *Oncology Letters.* 2012, 3(1), 163-171.

13. Zimmermann, C.; Tilghman, S. L; Boue, S. M; Salvo, V. A; Elliott, S.; Williams, K. Y.; Skripnikova, E. V.; Ashe, H.; Payton-Stewart, F.; Vanhoy-Rhodes, L. Fonseca, J. P.; Corbitt, C.; Collins-Burow, B. M.; Howell, M. H.; Lacey, M.; Shih, B. Y.; Carter-Wientjes, C.; Cleveland, T. E.; McLachlan, J. A.; Wiese, T. E.; Beckman, B. S.; Burow, M. E. *Journal of pharmacology and experimental therapeutics.* 2010, 332(1), 35-45.

14. Tilghman, S. L.; Boue, S. M.; Burow, M. E. *Molecular and Cellular Pharmacology*. 2010, 2(4), 155-160.

15. Salvo, V. A.; Boue, S. M.; Fonseca, J. P.; Elliott, S.; Corbitt, C.; Collins-Burow, B. M.; Curiel, T. J.; Srivastav, S. K.; Shih, B. Y.; Carter-Wientjes, C.; Wood, C. E.; Erhardt, P. W.; Beckman, B. S.; McLachlan, J. A.; Cleveland, T. E.; Burow, M. E. *Clinical Cancer Research*. 2006, 12(23), 7159-7164.

16. Wood, C. E.; Clarkson, T. B.; Appt, S. E.; Franke, A. A.; Boue, S. M.; Burow, M. E.; McCoy, Thomas; Cline, J. Mark. *Nutrition and Cancer.* 2006, 56(1), 74-81.

17. Payton-Stewart, F.; Schoene, N. W.; Kim, Y. S.; Burow, M. E.; Cleveland, T. E.; Boue, S. M.; Wang, T. Y. *Molecular Carcinogenesis.* 2009, 48(9), 862-871.

18. Kim, H. J.; Lim, J.; Kim, W.; Kim, J. *Proceedings of the Nutrition Society.* 2012, 71(1), 166-174.

19. Quadri, S. S.; Stratford R. E.; Boué; S. M.; Cole, R. B. *Analytical Chemistry*. 2013, 85(3), 1727-1733.

20. Gibson, G.; Skett, P. Introduction to Drug metabolism. Gibson, G. Skett, O. (Eds.) Blackie Academic and Professional, Champan & Hall, London. 1994.

21. Maarit, H.; Antti, H.; Kristiina, W.; Herman, A. *The Journal of steroid biochemistry and molecular biology* (2003), 87(4-5), 285-99.

22. Hu, Ming; Krausz, Kristopher; Chen, Jun; Ge, Xia; Li, Jianqi; Gelboin, Harry L.; Gonzalez, Frank. J. *Drug Metabolism and Disposition*. 2003, 31(7), 924-931

23. Chen, Jun; Lin, Huimin; Hu, M. *Cancer Chemotherapy and Pharmacology*. 2005, 55(2), 159-169. |

24. Hernandez-Montes, Eva; Pollard, Susan E.; Vauzour, David; Jofre-Montseny, Laia; Rota, Cristina; Rimbach, Gerald; Weinberg, Peter D.; Spencer, Jeremy P. E. *Biochemical and Biophysical Research Communications* .2006, 346(3), 851-859

25. Graf, B. A.; Ameho, C.; Dolnikowski, G. G.; Milbury, P.l E.; Chen, C.; Blumberg, J. B. *Journal of Nutrition* . 2006, 136(1), 39-44.

26. Yang, P.; Ebbert, J. O.; Sun, Z.; Weinshilboum, R. M. *Journal of Clinical Oncology*. 2006, 24(11), 1761-1769.

27. Liu, Y.; Hu, M. *Drug Metabolism and Disposition.* 2002, 30(4), 370-377.

28. Zhu, W.; Xu, H.; Wang, S.; Hu, M. *AAPS Journal.* 2010, 12(4), 525-536.

29. Bolling, B. W.; Court, M. H.; Blumberg, J. B.; Chen, C.Y. Oliver. *Journal of Nutritional Biochemistry*. 2010, 21(6), 498-503.

30. Boue, S. M.; Isakova, I. A.; Burow, M. E.; Cao, H.; Bhatnagar, D.; Sarver, J. G.; Shinde, K. V.; Erhardt, P. W.; Heiman, M. L. *Journal of Agricultural and Food Chemistry.* 2012, 60(25), 6376-6382.

31. Boué, S. M.; Isakova, I. A.; Burow, M. E.; Cao, H.; Bhatnagar, D.; Sarver, J. G.; Shinde, K. V.; Erhardt, P. W.; Heiman, M. L. J. *Agric. Food Chem*. 2012, 60 (25), 6376−6382.

32. Quadri, S. S.; Stratford R. E.; Boué; S. M.; Cole, R. B. "A New Mass Spectrometric Approach for Screening of Glyceollins and Their Metabolites" Proceedings of the 60th ASMS Conference on Mass Spectrometry and Allied Topics, Vancouver, BC, May 22, 2012.

33. Singh, Simendra; Khan, Amir R.; Gupta, Alok K. *Journal of Experimental Therapeutics and Oncology.* 2012, 9(4), 303-316.

34. Wu, Guoyao; Fang, Yun-Zhong; Yang, Sheng; Lupton, Joanne R.; *Turner, Nancy D. Journal of Nutrition.* 2004, 134(3), 489-492.

35. Dourado, Daniel F. A. R.; Fernandes, Pedro Alexandrino; Mannervik, Bengt; Ramos, Maria Joao. *Chemistry*. 2008, 14(31), 9591-9598.

36. Binkley, F. , and Nakamura, K. , *J. Biol. Chem.*1948, 173, 411.

37. Kera, Yoshio; Kiriyama, Takayuki; Komura, Setsuo. *Agents and Actions*. 1985, 17(1), 48-52.

38. Ketterer, Brian; Coles, Brian; Meyer, David J. *Environmental Health Perspectives*. 1983, 49, 59-69.

39. Boyland, E.; Williams, K.; *The Biochemical journal*. 1965, 94, 190-7.

40. Fjellstedt T A; Allen R H; Duncan B K; Jakoby W B. *The Journal of biological chemistry*. 1973, 248(10), 3702-7.

41. Shelnutt, S. R., Cimino, C. O., Wiggins, P. A., Ronis, M. J., & Badger, T. M. *The American journal of clinical nutrition*. 2002, *76*(3), 588-594.

42. Zhang, Y., Song, T. T., Cunnick, J. E., Murphy, P. A., & Hendrich, S. *The Journal of nutrition*. 1999, *129*(2), 399-405.

43. Zhang, Y., Hendrich, S., & Murphy, P. A. *The Journal of nutrition*. 2003, *133*(2), 399-404.

44. Gu, J. K., Zhong, D. F., & Chen, X. Y. *Fresenius' journal of analytical chemistry*. 1999, *365*(6), 553-558.

45. Bolling Bradley W; Court Michael H; Blumberg Jeffrey B; Chen C-Y Oliver. *The Journal of nutritional biochemistry*. 2010, 21(6), 498-503.

CHAPTER 3

ON-LINE THERMAL DESORPTION-GC-MS CHARACTERIZATION OF MICROBIAL VOLATILE ORGANIC COMPOUNDS DETECTED FROM SIMULATED FLOODING ENVIORNMENTS AND PRODUCED BY *CHAETOMIUM* AND *CLADOSPORIUM* FUNGI

Syeda S. Quadri, Michael Ferris, Jim Cutler, Richard B. Cole

3.1 Abstract

Mold infestation is a global problem associated with damp environments. Mold produces microbial volatile organic compounds (MVOCs) that can vary depending on the implicated fungal species and the growth substrate. In this paper, the presence of fungi and their MVOC production was monitored from different simulated flooding environments employing freshwater, brackish, and saltwater. The MVOCs were analyzed using a modern technology system coupling thermal desorption on-line with gas chromatography-mass spectrometry (TDA-GC-MS). 1-Undecanol, 2-ethylhexanal, and 2-ethylhexanol were found to be present in all simulated flooding environments. However, no specific pattern in MVOCs production was observed that was dependent on the salinity. Molecular identification of fungi was also performed and 10 species were identified. Included in the identified fungi are *Cladosporium cladosporioides, Dothideomycetes sp, Chaetomium murorum*, and *Fusarium delphinoides* that are commonly associated with damp environments. Guided by the above findings, toxic fungi *Chaetomium sp.* and *Cladosporium sp.* were cultivated on drywall (low nutrient) or potato dextrose agar (PDA, high nutrient) substrates and MVOCs produced from these fungi were compared to determine the effects of substrate on MVOC production and to identify novel MVOCs that are indicative of growth for each fungus. 3-Furaldehyde and 3-(4-hydroxy-3-methoxyphenyl)-2-propenal were consistently detected in both growth media for each of the mold species. Thus, we propose these latter two MVOCs as novel indicators of mold growth for *Chaetomium sp.* and *Cladosporium sp* fungi.

3.2 Introduction

Flooding of human dwellings is a global problem and many uncertainties exist concerning the assessment of human health risks associated with exposure to consequent mold growth. Hurricane Katrina struck New Orleans on August 29th 2005, and in the aftermath following multiple levee breakages, 80% of the city became flooded with water levels as high as 6 m (1). Approximately 120,000 homes were flooded and some homes remained under water for several weeks (2). Because of the widespread flooding, there was extensive mold growth in the flooded areas. A survey conducted by the Centers for Disease Control and Prevention showed that 46% of randomly selected houses in the New Orleans area had visible mold growth and 17% had heavy mold contamination (3). As determined by indoor and outdoor air sampling, the predominant mold species present in the contaminated houses were *Aspergillus, Cladosporium, and Penicillium* (3,4); *Stachybotrys* was also found in some houses (2). This became an immediate concern because adverse public health effects have been associated with species belonging to these genera. (2,5,6,7). The adverse health effects include pulmonary, immunologic, neurologic, and oncologic disorders (5). Various illnesses caused by mold include airway infections, compromised immune function, bronchitis, asthma, and extreme fatigue (7, 5, 13).

Fungi affect human health through well-defined mechanisms: generation of harmful immune response, direct infection by the microbe, and toxicity/irritation from by-products (27). Among the toxic irritants are secondary metabolites that are produced for species protection and to promote sporulation (8). Secondary metabolites may also be produced during nutrient deprivation, or in the presence of competing coexisting species or environmental stressors (21). Secondary metabolites produced by fungi include mycotoxins and volatile organic compounds. Referred to as microbial volatile organic compounds (MVOCs), these are small-molecules that are

produced as end products of the metabolism of organic material (9, 21). Elevated amounts of indoor MVOCs create a potential health hazard to humans (10, 11). While some studies suggest that there is no correlation between fungal MVOCs and human health, other studies link MVOCs to an increase in nasal lavage biomarkers, frequent blinking and a decrease in forced vital capacity (FVC) (12, 13). MVOCs are also associated with "sick building syndrome." (15) The latter refers to a 'higher than normal' prevalence of symptoms affecting the eyes, head, upper respiratory tract and skin associated with a particular building (36,37).

Visual mold growth is an obvious indication of the presence of mold. However, only 10-20% of the mold in an affected building is typically visible (16). Often mold remains hidden behind shelves, carpets, wallpaper, wardrobes or covered ceilings. Hidden mold can be detected by analysis of material collected from surfaces, or by sampling and analysis of MVOCs (16). The analysis of MVOCs is typically carried out by first capturing MVOCs on an adsorbent using active or passive sampling. The collected analytes can be extracted from the adsorbent by either classical solvent extraction or by the newer approach of thermal desorption (29,30). In thermal desorption, trapped volatiles and semi-volatiles are released from adsorbents by rapid heating with recapture of the desorbed products on a cold trap. Afterwards, the cold trap is rapidly heated in preparation for the analysis step. The thermal desorption technique provides the advantage of eliminating the solvent dilution step of conventional solvent extraction procedures. By avoiding a solvent extraction step, the extraction efficiency of thermal desorption can approach 100% from porous polymer or charcoal sorbents (29).

A well-established (39,40) approach for volatile and semi-volatile analysis is the combination of gas chromatography (GC) separation followed by electron ionization mass spectrometry (EI-MS) detection. The rapid desorption from the cold trap of a Thermal Desorption

Analyzer (TDA) is highly compatible with the requirement to introduce all desorbed species onto the GC column in a narrow band. The powerful combination of TDA-GC-EI-MS is a very convenient, sensitive and selective approach for trapped volatile and semi-volatile analysis that has been gaining increasing attention in recent years (22,23).

The combination of TDA-GC-EI-MS has been used to analyze environmental air samples from various mold growth scenarios. Researchers have proposed that certain MVOCs (mainly aldehydes, alcohols, ketones, furans and terpenes) can be used as indicators of mold contamination in indoor environments (21). Chemical markers which have been reliably connected to fungal growth include 3-methylfuran, octan-3-one, hexan-2-one, heptan-2-one, 1-octen-3-ol, 3-octanol, and 3-octanone among others (14, 17, 18, 19, 35). The MVOCs 1-octen-3-ol and 3-methylfuran have been suggested to cause acute irritation to the eyes, throat, and respiratory airways (14,38). However, much of the MVOC data that can be found in the literature concerning flooded environments was assessed months after the actual flooding event (18, 22, 23, 24, 25, 28). Other MVOC analyses have investigated emissions from individually cultivated fungal species that were usually chosen based on suspected toxicity of the fungus (18, 22, 23, 24, 25, 28).

The study described in this paper uses an integrated two-pronged approach to assess MVOC production from fungal species appearing in flooded environments. Flooding events simulating actual flooding conditions in southern Louisiana (using different water salinities) were carried out in glass containers. MVOC analyses of volatiles and semi-volatiles were performed as was DNA sequence analysis of visible fungal growth. Toxic fungi identified by DNA sequencing were then investigated in isolation. MVOCs of cultivated fungi and simulated flood fungi were compared. The aim of the present study is uncover unique MVOCs of fungi that can serve as diagnostic MVOCs to establish the type of mold present in damp environments.

3.3 Method and Materials

3.3.1 Simulated flooded environment

Flooded home simulations were created in one-gallon glass containers. Each container held a 6 x 4-inch piece of gypsum board that was "flooded" with one liter of either brackish, fresh, or salt water. Another container was flooded with freshwater to which plant food was added to investigate the effects of nutrients. Brackish water was obtained from Lake Pontchartrain, LA (accessed from New Orleans near Elysian Fields Blvd.), whereas freshwater and saltwater were obtained from the Mississippi River (accessed from Kenner, LA near Williams Blvd.) and Saint Louis Bay (accessed from Slidell, LA), respectively. The containers were closed with lids and were set in a greenhouse where temperatures reached above 90 ^{o}F during the summer. Four openings were drilled in the lids of the glass containers for air intake and sampling. A glass tube filled with glass wool was placed in the air inlet to reduce circulation and to prevent a vacuum from being created during the air sampling period. The other 3 openings were used to hold sorbent tubes during air sampling; these openings were closed with cork at all other times.

3.3.2 MVOC sampling of simulated flood chambers

Microbial volatile organic compounds were collected on days zero, four, nine, and fourteen. Volatile sampling was carried out using AirChek 52 pumps (SKC Gulf Coast Inc, Houston, TX). Low flows were maintained by a Tri Adjustable Low Flow Holder (Gulf Coast Inc, Houston, TX). Three sorbent tubes, 4 ½" x 4 mm ID packed with Carboxen 1000, Carbosieve SIII, and Tenax-TA (CDS Analytical Ins, Oxford, PA), were placed on the lids of each container that were connected to a pump through the tri-manifold. All samples were collected in triplicate. Volatile sampling was performed for 60 min at the flow rate of approximately 8.3 mL/min for a total (calibrated) sampling volume of 0.5 L per tube. The three replicates allowed a total of 1.5 L

of air to be sampled per container. EPA method TO-17 recommends limiting volumes to 0.5 L per tube when water is present or to 2 L when there is only high humidity (30). Each time that volatile sampling was performed, greenhouse air and lab air were also collected to serve as controls.

3.3.3 On-line thermal desorption-gas chromatography-ion trap mass spectrometry

The sorbent tubes used for volatile sampling of the simulated flooded environments were thermally desorbed at 300 ºC for 15 min using a Dynatherm 9300 thermal desorption analyzer (TDA) (CDS Analytical Inc, Oxford, PA). After recapture on the "trap" of the TDA, this trap was heated at 310 ºC for 5 min to desorb all MVOCs into the transfer line leading to the GC-MS. GC transfer line and interconnect line temperatures were kept at 300 ºC. Helium was used as the carrier gas at a flow rate of 60 mL/min for thermal desorption. The injection port temperature of the GC (Varian 450 GC, Walnut Creek, CA) was kept at 250 ºC with injections performed in split mode using an injection ratio of 1/20. The GC carrier gas flow rate was 1.0 mL/min. The oven temperature was programmed from 40 ºC to 250 ºC at 8 ºC/min with a hold time of 5 min. The initial hold time of the oven was 2 min. The MS (Varian 240 MS, Walnut Creek, CA) transfer line temperature was 280 ºC. Samples were analyzed in EI mode using 70 eV electron energy. A 2 min post-injection filament delay was used, during which time no data was acquired on the mass spectrometer. To qualify as a detected signal, a signal-to-noise ratio of greater than 3 was required in the obtained EI mass spectrum. The NIST library was used to identify eluted compounds. These identifications were confirmed by manual interpretation of mass spectra. When the spectrum of the library did not match closely with the spectrum of the compound detected, the compound was treated as an unknown. This method is based upon EPA TO-15 (32) with slight modifications.

3.3.4 Mold collection and identification

Samples of the individual mold colonies that were imbedded on the drywall were obtained by removing a speck with sterile tweezers. The samples were placed in microcentrifuge tubes. Fungal DNA was obtained using the commercially available fungal genomic DNA kit "MasterPure^{TM} Yeast DNA Purification Kit" (Epicenter Biotechnologies, Madison, WI). Genetic identification of fungal species was performed using polymerase chain reaction (PCR) assays directed towards a broad range of fungal genera. PCR-amplification with ITS4 and ITS5 primers was carried out in a thermocycler (BioRad, Hercules, CA). These primers, as described by White et al. (31), amplify the conserved regions of 28S (ITS 4) and 18S (ITS 5) rRNA genes. Sequences of primers are as follows: ITS 4, 5'-TCCTCCGCTTATTGATATGC-3' and ITS 5, 5'-GGAAGTAAAAGTCGTAACAAGA-3'. Thermal cycling consisted of 95^{o} C for 4 min, followed by 30 cycles of 95 ^{o}C for 1 min, 52 ^{o}C for 1 min, and 72 ^{o}C for 1 min, and final extension at 72 ^{o}C for 7 min. The sequencing reaction was performed by Davis Sequencing, Inc (Davis, CA) and sequence analyses and alignments were carried out using Sequencher Software. The BLAST algorithm at the NCBI website was used to identify the fungal sequences.

3.3.5 Laboratory cultivation

Two nutrient media were used, either gypsum board (drywall, low nutrient) or potato dextrose agar (PDA, high nutrient). Gypsum board was selected because it is the most common wall building material in the New Orleans region, whereas PDA was employed because it is the most commonly used laboratory medium for cultivation of fungi. Potato dextrose agar plates were prepared by autoclaving 9.75 g of PDA in 250 mL of deionized water. Drywall plates were made the same way, except that drywall was pulverized and suspended in the agar. The plates were cooled and stored at 4 ^{o}C until inoculation. *Chateomium* (M1.903) and *Cladosporium* (M1.881)

were separately inoculated on petri plates on both media. The petri plates were stored at 4 ^{o}C for at least one week before inoculation, so that any media gaseous emission would not interfere with MVOCs sampling. After inoculation, the petri plates were placed in cultivation chambers (one-gallon glass containers similar to those used for simulated floods) with four openings on screw-top lids. One opening of each container was fitted with glass wool-packed glass tubes for air exchange, whereas the other three were closed when sampling was not being performed. Containers were left to incubate for 20 days before sampling for MVOCs. Volatiles sampling for these cultivated fungi was carried out in a manner analogous to what was described above for simulated flooded environments. TDA-GC-EI-MS conditions employed for volatile analyses were also the same as those used for simulated floods.

3.4 Results and Discussion

The first part of our study employs simulated flooding environments to investigate mold growth and MVOCs production over time in the presence of coexisting species. Flood conditions were simulated by the use of fresh or salt water to investigate the species of mold that proliferate on gypsum board building material. Gypsum board, commonly known as drywall, is primarily a source of carbon as well as co-factors such as Ca^{2+}, K^{+}, and other nutrients. Nutrients for mold growth are usually also present in flood water; moreover, nitrogen fixing bacteria present in the environment, can provide a source of fixed nitrogen needed for fungal growth. In New Orleans, flooding of homes by freshwater is common. Such floods are often due to intense rain events that overwhelm pumping station capacities. In nearby areas, freshwater flooding caused by intense rain and high river levels is also common. On the other hand, the storm surge associated with hurricane causes salt water flooding along coastal communities in Louisiana. For this reason, variable salinity levels were employed in our simulated flooding to probe the effects of salt content on the variety of mold species that proliferate and the types of MVOCs that are produced in flooded environments.

3.4.1 PART I: MVOC analyses of simulated flood environments

Statistically significant amounts of MVOCs were detected by Day 4 of sampling. The variety and quantities of MVOCs were monitored over time. Table 3.1 lists MVOCs detected over three different sampling periods along with their relative peak areas. The changes in the peak areas over a two week time period allowed calculation of the temporal variation in concentration of each MVOC. No *visible* mold growth was observed during the two week period; however, MVOC data indicates that mold growth activity was occurring. A few of the detected and identified MVOCs have been reported in the literature as mold indicators, such as

Type of flooding environment	River (freshwater)			Bay (salt water)			Lake (brackish)		
Time of MVCOs sampling (days)	Day 4	Day 9	Day 14	Day 4	Day 9	Day 14	Day 4	Day 9	Day 14
MVOCs	Peak areas given in arbitrary units								
3-Furaldehyde	$7.0x10^7$	nd	nd						
2,2-diethyl-3-methyloxazolidine	$5.6x10^6$	nd	nd						
I-Undecanol	$4.9x10^6$	$1.3x10^6$	$1.0x10^7$	$4.5x10^6$	nd	$1.2x10^7$	$5.1x10^6$	nd	nd
3-Hexen-2,5-diol	nd	nd	$3.4x10^6$						
4-Methoxy-4-vinylphenol	$2.5x10^7$	nd	nd						
2-Ethylhexanal	$1.1x10^7$	$7.4x10^5$	$2.4x10^6$	$1.4x10^7$	$8.0x10^5$	$1.4x10^7$	nd	$2.7x10^7$	nd
2-Ethylhexanol	$5.4x10^5$	$8.9x10^6$	$1.0x10^7$	$3.0x10^7$	$8.5x10^5$	$4.3x10^7$	$9.2x10^7$	$5.2x10^7$	$3.2x10^7$
Vanillin	$2.7x10^7$	nd	nd						
4-Phenylcyclohexene				nd	nd	x			
1-(2-methylpropyl)-cyclohexene						$5.3x10^6$	$2.9x10^6$	$1.5x10^6$	$1.3x10^6$
3-Heptanone				$6.9x10^5$	nd	$2.8x10^5$			
2-Methyl-3-hydroxy-2,4,4-trimethylpentyl ester propanoic acid	$8.1x10^6$	$3.5x10^6$	$7.5x10^6$	$1.0x10^7$	nd	$7.1x10^6$	$1.4x10^7$	$8.7x10^6$	$1.0x10^7$
Thujopsene-13	nd	nd	$9.9x10^6$	nd	nd	$7.8x10^6$			
3-Heptanol				nd	nd	$1.1x10^5$	nd	$3.0x10^7$	nd
3-(4-hydroxy-5-methoxyphenyl)-2-propenal	$4.0x10^7$	nd	nd						
2-Heptanone	$2.2x10^5$	nd	nd						

Table 3-1: Peak areas of MVOCs found from freshwater, salt, and brackish water simulated floodings. "nd" indicates not detected.

2-heptanone, 2-ethylhexanol, and 1,1a,4,4a,5,6,7,8-octahydro-2,4a,8,8,tetramethyl-,(1aS,4aS,8aS)-(-)-cyclopropana[d]naphthalene (thujopsene). (23) While some MVOCs unique to each environment were noted, many MVOCs were observed consistently in 2 of the 3 flooding conditions or even in all 3 of the flooding conditions. 2-Ethylhexanal, 2-ethylhexanol, 1-undecanol, 2-Methyl-3-hydroxy-2,4,4-trimethylpentyl ester propanoic acid were common to all three flooding conditions. By contrast, thujopsene was detected from freshwater and saltwater simulated flooding, whereas 3-heptanol was detected from saltwater and brackish water flooding. Thujopsene-13 was not detected from either medium until day 14, while 3-heptanol was detected on day 9 from brackish and day 14 from saltwater flooding in high abundance. Some of the freshwater MVOCs were also detected from the saltwater and brackish water, but many more MVOCs were detected from freshwater simulated flooding. 4-phenylcyclohexene and 3-heptanone were specific to saltwater, whereas 1-(2-methylpropryl)-cyclohexene was found only in brackish water. On the other hand, 3-furaldehyde, 2,2-diethyl-3-methyloxazolidine, vanillin, 3-(4-hydroxy-5-methoxyphenyl)-2-propenal, and 2-heptanone were specific to freshwater simulated flooding.

From the above mentioned MVOCs, thujopsene and 2-ethyl-1-hexanol are MVOCs produced by *Stachybotrys chartarum* (23). In particular, 2-ethyl-1-hexanol was reported to be readily produced by *Stachybotrys chartarum* on drywall board cultures (23). The detection of these two compounds in the freshwater flooded environment suggests the presence of *Stachybotrys chartarum* under these flooding conditions. 2-Heptanone, which is often reported as a mold growth marker, was only detected from freshwater MVOC sampling. It is reported to produced by *Aspergillus sp, Penicillium sp., Eurotium sp, Chaetomium globosum, and Cladosporium cladosporoides* (9,14,25,26). Thus, it is likely that one or more of these species is present in the

freshwater simulated flooding environment. Our results also suggest that the freshwater environment allows proliferation of many coexisting species as compared to higher salinity conditions. Because mold growth was not visible to the naked eye by day 14 of simulated flooding, we consider MVOC analysis to be a more effective approach for monitoring the start of mold growth activity.

3.4.2 PART II: Molecular identification and MVOC results and discussion

Research has shown that the use of PCR-amplification and DNA sequence analysis of fungal internal transcribed spacer (ITS) regions provides a highly complete and accurate assessment of fungi present in natural specimens (33,34). For this reason, the PCR-amplification DNA sequencing approach was used in our study. Mold appearing in colonies was scraped from above the "water line" in each of the three simulated flood environments. Samples for molecular identification were taken on days 40 and 70. The sequencing results suggested mixed populations of fungi were present. Mixed populations were observed from every simulated flood environment. The sequencing data of the first fungal colony sampling (day 40) indicate that the freshwater flooded environment had *Cladosporium cladosporioides* and *Toxicocladosporium irritans* colonies. Drywall flooded with the brackish water showed *Helotiales sp*. growth along with an unknown fungus which did not match any sequence from BLAST. While *Cladosporium* genus was detected from freshwater flooding, other expected molds such as *Aspergillus, Penicillium, and Stachybotrys* were not observed. It was surprising to see that sampling results showed no appearance of the most predominantly reported mold species associated with damp buildings, i.e., *Aspergillus* and *Penicillium* (2-7). Linking these identifications to the findings in Part 1, the detection of 2-heptanone can be attributed to the presence of *Cladosporium cladosporoides* in freshwater flooding.

At the second fungal sampling (day 70), *Dothideomycetes sp* was predominantly found from both brackish and freshwater flooding. Regardless of salinity, the fact that one predominant species (*Dothideomycetes sp*) was observed after 2 months suggests that it utilizes the available resources effectively, hence, it proliferates even when nutrients are scarce. *Dothideomycetes sp* are known to effectively degrade biomass and contribute to the carbon cycle (45). They are also tolerant of extreme environments such as heat, humidity, and cold (46). Because the experiment lasted for over two months, a diminishing amount of nutrients remained present in the containers over time. Since *Dothideomycetes sp* is capable of fixing its own carbon source and can survive harsh conditions, this may account for its advantage in proliferating over other species.

A simulated flood of freshwater, to which plant food (with additional nutrients) was added, showed considerably more fungal species on the second fungal sampling (day 70) compared to plain freshwater which showed considerably less visible mold. When searching the BLAST database, our obtained sequencing data of the first fungal sampling (day 40) identified the presence of *Cladosporium cladosporioides, Cochliobolus lunatus* and *Dothideales sp.*, whereas the second fungal sampling results (day 70) identified *Scedosporium dehoogii, Chaetomium murorum, Fusarium delphinoides, Cochliobolus lunatus*, and an unknown. . Importantly, *Cladosporium cladosporioides, Chaetomium murorum* and *Fusarium delphinoides* are toxigenic molds that have been associated with human health risk. *Chaetomium sp*. can cause onychomycosis, peritonitis, empyema, pneumonia, and invasive/cerebral disease in immuno-compromised persons (41). *Fusarium sp.* has been linked to allergies, wounds and infections of the eyes and fingernails, invasive mycoses, inhalation and deep skin incisions to people with weak immune systems (42). *Cladosporium sp.* are known to cause ergotism and chronic hypersensitivity pneumonitis (HP)

(43). The sources of these fungal species found in BLAST were soil, water, or moldy paint. These results suggest that in the presence of more available nutrients, many fungal species can coexist.

MVOC sampling was performed prior to each colony sampling for fungal sequencing. The MVOCs detected from the freshwater simulated flooding with added nutrients (day 40) include 2-hexen-1-ol, cyclohexanone, 2,2,6-trimethylcyclohexanone, octanal, and 2,5-diphenylbenzoquinone. Wilkins et al. (22) found octanal in the dust and material obtained from a moldy building, but it was not detected in their air sampling. In the current study, octanal was detected from the air of the freshwater simulated flood. Cyclohexanone has been reported to be produced by *Cladosporium cladosporioides, Aspergillus versicolor, A. niger, A. fumigatus,* and *Penicillium expansum* (26). As mentioned above, the genetic sequencing data shows the presence of *Cladosporium cladosporioides.* Thus, cyclohexanone could have been produced by *Cladosporium cladosporioides.* While day 40 showed the presence of several MVOCs from freshwater simulated flooding with added nutrients (plant food), no significant amounts of MVOCs were detected on day 70. Furthermore, significant amounts of MVOCs were not detected from other simulated environments for either sampling period. The number of MVOCs detected at the later stage (days 40 and 70) of flooding was much lower than that detected at the earlier stage (days 4-14). This may be a reflection of the diminishing availability of nutrients as time progressed, causing a decrease in mold growth and associated MVOC production.

Another volatile sampling was performed 4 months (day 120) after the simulated flooding. Although mold growth was visible, no MVOCs were detected in any of the simulated flood environments. These results were in accordance with the first set of simulated flooding results (day 70). Many cultivation studies propose that the largest amounts of MVOCs are produced at the beginning of cultivation (9). Mold undergoes exponential growth for 3 days after inoculation and

then switches its metabolism to idiophase (stationary phase) to produce spores and MVOCs. Much of the cultivation medium is consumed in 15 days (9), so MVOC production decreases. This may be the case in the simulated flood where over time, fungi proliferate and eventually a nutrient deficiency occurs. At that point, mold can no longer undergo idiophase metabolism to produce MVOCs.

3.4.3 PART III: MVOCs detected from cultivation of fungi

Cladosporium sp. and *Chaetomium sp.* fungi were chosen for cultivation since they were found in simulated floods and they are often associated with damp environments. Several volatiles were detected from the *Chaetomium sp.* and *Cladosporium sp.* growth cultivated in nutrient-rich medium (PDA) and low nutrient medium (drywall) including several alcohols, aldehydes, ketones, and furans that have been suggested to be mold growth indicators. Table 3.2 shows the complete list of volatiles found from the two species on both growth media.

MVOCs observed from *Chaetomium sp* cultivated on the nutrient-rich medium include 3-octanol, 3-octanone, 3-furaldehyde and 3-(4-hydroxy-3-methoxyphenyl)-2-propenal. The last two MVOCs mentioned were consistently observed from both *Chaetomium sp.* and *Cladosporium sp.* regardless of the substrate. *Chaetomium* genus, and in particular *Chaetomium globosum* produce 3-octanone and 3-octanol that are commonly associated with mold growth (9). However, the latter two common mold growth indicators were not detected from drywall medium. Tiebe et al. (24) and Matysik et al. (26) each detected production of 3-octanone from cultivation of fungi on nutrient-rich media DG 18 agar and malt extract agar (MEA), respectively, along with many other MVOCs. Gao and Martin (23) compared the production of 3-octanone from gypsum board with MEA and reported its occurrence from MEA medium only. The absence of 3-octanone from low nutrient media thus seems general, and it indicates that this volatile is more likely to appear when

mold proliferates in a nutrient-rich environment. For this reason, 3-octanone may not be a good 'global' mold growth indicator in all environments.

In comparison with *Chaetomium sp., Cladosporium sp.* produced a greater number of volatile organic compounds on the nutrient rich medium. The MVOCs produced by *Cladosporium* included several aldehydes, ketones, furan, nitrogen containing compounds and a few unknowns (see Table 3.2). MVOC 3,3,5-trimethylcyclohexanone was of particular interest since its isomer 2,2,4-trimethylcyclohexanone was detected from the freshwater simulated flooding with added nutrients. As mentioned above, the genetic sequencing data showed that one of the species found from freshwater simulated flooding with added nutrients was *Cladosporium cladosporioides.* The detection of one of two trimethylcyclohexanone isomers from either the simulated flooding with added nutrients or cultivation of *Cladosporium sp.* on PDA medium suggests that fungi produce certain unique volatiles when provided with nutrient-rich environments. Because neither trimethylcyclohexanone isomer was detected from the drywall medium, they cannot be used as biomarkers for *Cladosporium sp.* This underscores the fact that production of MVOCs is strongly dependent on the available nutrients.

MVOCs found from *Chaetomium sp.* growth on low nutrient medium include styrene, 3-furaldehyde and 3-(4-hydroxy-3-methoxyphenyl)-2-propenal along with 3-pyridinol and 2,2-diethyl-3-methloxazolidine; the latter two contain nitrogen. 3-furaldehyde and 3-(4-hydroxy-3-methoxyphenyl)-2-propenal were also detected from *Cladosporium sp.* growth on low nutrient medium. Amine containing volatiles were not detected, but every MVOC that was detected from *Cladosporium sp.* growth on low nutrient medium was also observed from nutrient-rich medium. The absence of many volatiles from *Chaetomium sp.* growth on low nutrient medium as compared to nutrient-rich medium (see Table 3.2) indicates again that the production of MVOCs is highly

dependent on the growth substrate. Other studies have also mentioned that specific MVOC production changes with the medium (20,23,25). Styrene has been reported as a MVOC produced by *Penicillium* and *Trichoderma* (20, 25). The results of our study show that styrene is also produced by *Chaetomium* even in a nutrient-deprived environment.

Table 3-2: List of MVOCs produced by *Chaetomium sp.* and *Cladosporium sp.* on PDA and drywall media. "nd" indicates not detected

Microbial Volatile Organic Compounds	*Chaetomium*		*Cladosporium*	
	PDA	Drywall	PDA	Drywall
	Peak areas given in arbitrary units			
3-furaldehyde	$7.18x10^6$	$2.24x10^6$	$1.12x10^7$	$4.38x10^6$
3-(4-hydroxy-3-methoxyphenyl)-2-propenal	$1.02x10^7$	$2.97x10^6$	$2.81x10^7$	$6.37x10^6$
3-Octanone	$1.54x10^6$	nd		
3-Octanol	$1.31x10^6$			
2,2-diethyl-3-methloxazolidine	nd	$7.90x10^6$	$5.26x10^6$	
3,3,5-Trimethylcyclohexanone			$1.02x10^6$	
3-Pyridinol	nd	$2.24x10^6$	$1.94x10^6$	
Styrene	nd	$7.62x10^6$		
Vanillin			$8.41x10^6$	
2-Furanmethanol			$9.85x10^5$	
Unknown M+. 162			$1.19x10^7$	$4.55x10^6$
Unknown M+. 114			$1.17x10^7$	

No MVOC could be called a biomarker of either *Cladosporium sp.* or *Chaetomium sp.* because no single volatile was detected from the same fungus grown on both media. Nonetheless, 3-furaldehyde and 3-(4-hydroxy-3-methoxyphenyl)-2-propenal were consistently observed from either growth medium for both of the mold species. Figures 3-1 and 3-2i show the electron ionization mass spectra of these MVOCs along with the NIST library match. The spectra were also manually interpreted to confirm the MVOCS. Figure 3-3 and 3-4 show the decomposition mechanism of 3-furaldehyde and 3-(4-hydroxy-3-methoxyphenyl)-2-propenal, respectively. Many substituted furans and substituted propenals have been detected from damp buildings, but to our knowledge these two compounds have not been reported as mold MVOCs in the literature. We thereby propose 3-furaldehyde and 3-(4-hydroxy-3-methoxyphenyl)-2-propenal as novel indicators of mold growth of *Chaetomium sp* and *Cladosporium sp* fungi.

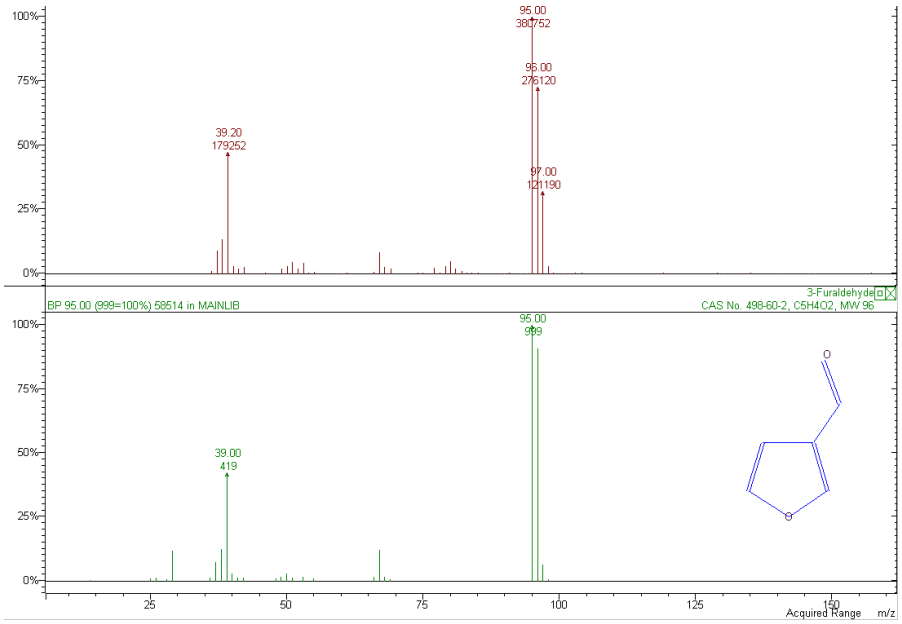

Figure 3-1: EI Mass spectra of 3-furaldehyde. Top spectrum is obtained from MVOC sampling of cultivated fungal species. Bottom spectrum is the NIST library match of 3-furaldehyde.

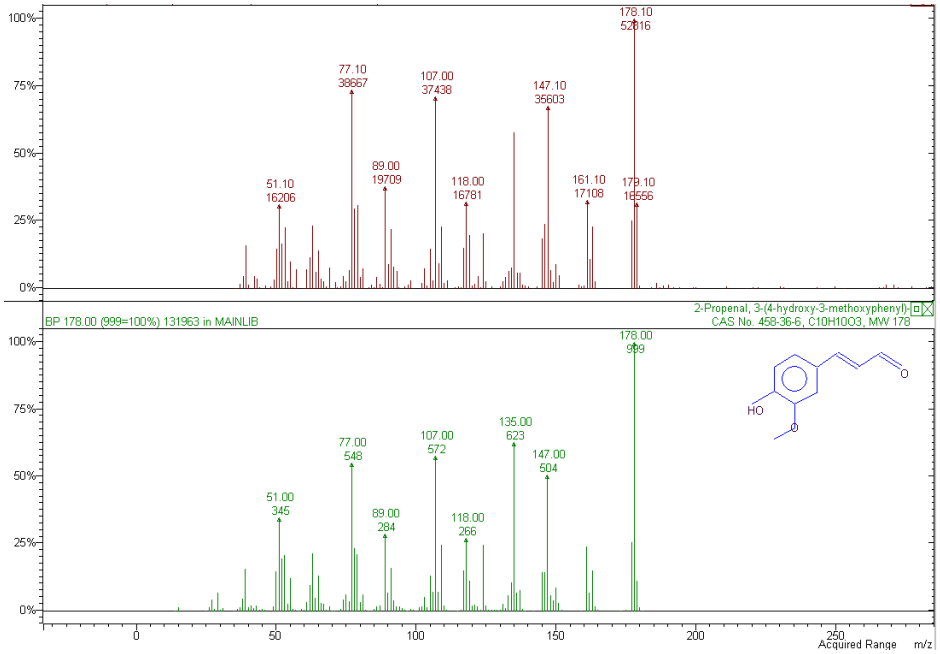

Figure 3-2: EI mass spectra of 3-(4-hydroxy-3-methoxyphenyl-2-propenal. Top spectrum is obtained from MVOC sampling of cultivated fungal species. Bottom spectrum is the NIST library match of 3-(4-hydroxy-3-methoxyphenyl-2-propenal.

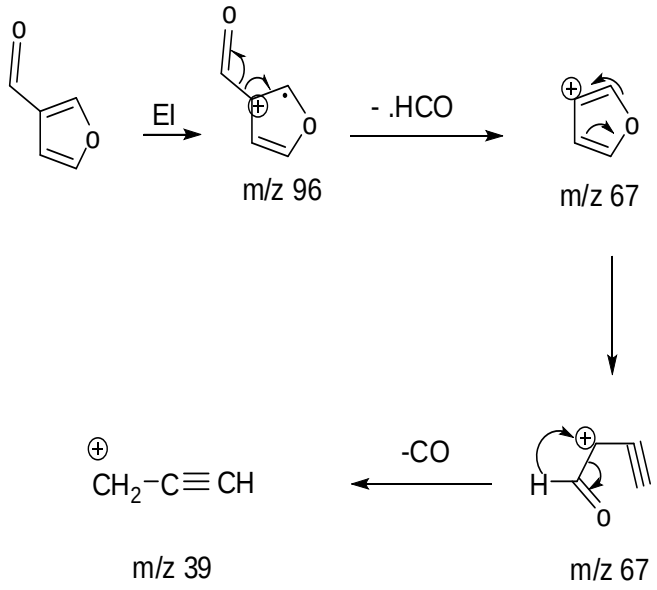

Figure 3-3: Decomposition mechanism of 3-furaldehyde.

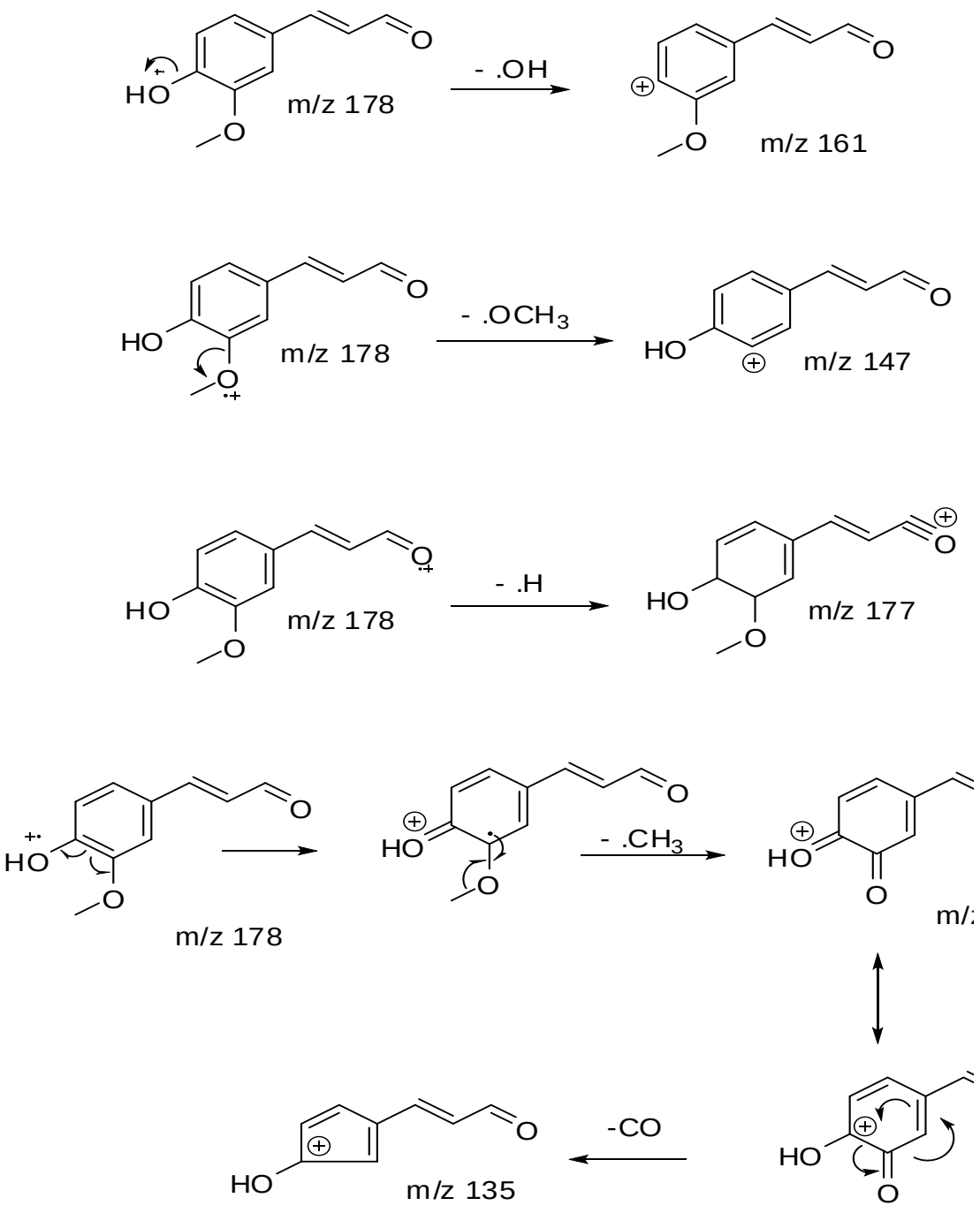

Figure 3-4: Decomposition mechanism of 3-(4-hydroxy-3-methoxyphenyl)-2-propenal.

3.5 Conclusion

TDA-GC-MS analyses were carried out to identify MVOCs from fungi that coexist in simulated flooding environments, as well as from fungi cultivated in isolation that were identified in these simulated flooding environments. High abundances of MVOCs were detected in the early stages (between days 4-14) of simulated flooding, even when no fungal growth was visible to the naked eye. This strongly suggests that MVOCs are produced when fungi are actively proliferating. By Day 40, and continuing afterwards, no significant amounts of MVOCs were detected from saltwater, brackish, and freshwater flooding environments even though mold was visible in all simulated environments. The salinity of the flood water did not show a clear correlation with production of a specific type of MVOC.

Low abundances of MVOCs were found on Day 40 only from the freshwater flooding environment to which plant food was added. Furthermore, in this latter nutrient-rich environment only, the continuous presence of several fungal colonies was observed even at Day 70, suggesting that when nutrients are available, a greater number of fungal species continue to grow. Notably, no MVOCs were detected from any environment on Day 70 or Day 120. These results clearly demonstrate that the decrease in MVOC production over time is highly dependent on fungal growth stage. Another temporal aspect of mold growth that was deduced from molecular identification data, was the change in the number of species present. After 40 days of flooding, multiple fungal species were identified, but at Day 70, one species was found to be dominant (*Dothideomycetes sp*.) in freshwater and brackish water simulated flooding.

Cultivation data from *Chaetomium sp.* and *Cladosporium sp* indicate the production of a higher number of MVOCs on PDA compared to dry wall. Not all MVOCs that are produced under the former nutrient-rich environment are produced on the latter low-nutrient environment. The

MVOCs of particular interest to us that were detected from simulated flooding include 2-heptanone, 3-furaldehyde, 2,2-diethyl-3-methyloxazolidine, and 3-(4-hydroxy-5-methoxyphenyl)-2-propenal. 2-Heptanone is notable because it has been previously proposed as a mold growth indicator and it is produced by several toxic fungi including *Cladosporium cladosporioides.* The latter fungus was shown by genetic sequencing data to be present in the freshwater flooding with added nutrients environment along with other mold species. MVOC sampling from this environment showed the presence of 2-heptanone that was likely produced by *Cladosporium cladosporioides*.

Other MVOCs 3-furaldehyde, 2,2-diethyl-3-methyloxazolidine, and 3-(4-hydroxy-5-methoxyphenyl)-2-propenal were observed from the freshwater simulated environment (where *Cladosporium sp* was detected) and from cultivation of *Cladosporium sp.* and *Chaetomium sp.* 3-Furaldehyde and 3-(4-hydroxy-5-methoxyphenyl)-2-propenal were consistently observed from the freshwater flooding environment, as well as PDA and drywall cultivation of both *Cladosporium sp*. and *Chaetomium sp.* By contrast, 2,2-diethyl-3-methyloxazolidine was detected only from freshwater flooding, *Cladosporium sp* cultivated on PDA and *Chaetomium sp.* cultivated on drywall. Because 2,2-diethyl-3-methyloxazolidine was not detected from all media, it cannot be used as a reliable biomarker for these fungi. On the other hand, 3-furaldehyde and 3-(4-hydroxy-5-methoxyphenyl)-2-propenal that were consistently observed from *Cladosporium sp.* and *Chaetomium sp.* when grown in isolation, can serve as indicators of *Chaetomium* or *Cladosporium* growth.

The use of TDA-GC-MS for MVOC detection is a convenient method to identify the presence of fungi in moldy buildings especially because this technique has the advantage of detecting hidden fungal growth. MVOC analyses and genetic identification using PCR

amplification are two complementary methods. PCR amplification and sequencing is time consuming, but it is a reliable method for identifying the type of mold present when mold is visible to the naked eye. On the other hand, MVOC analysis leads to a more rapid indication of fungal species at an earlier stage of development (i.e., even before mold growth becomes visible) compared to cultivation or sequence analysis.

3.6 References

1. Knabb, R.D., Rhome, J.R., and Brown, D.P., 2005. NOAA National Hurricane Center. 20 Dec., 2005.

2. Solomon, Gina M.; Hjelmroos- Koski, Mervi; Rotkin- Ellman, Miriam; Hammond, S. Katharine. Environmental Health Perspectives (2006), 114(9), 1381- 1386.

3. Centers of Disease Control and Prevention. MMWR. Morbidity and mortality weekly report (2006), 55(2), 41- 4.

4. Ratard, R., Brown, CM, Ferdinands, J., Callahan, D., Dunn, KH, Scalia, MR, et al. Morbidity and Mortality Weekly Report (2006), 55:2, 41- 44.

5. Ashraf, Hossain; Sotohy, Ahmed; Afif, G. The Journal of allergy and clinical immunology (2004), 113(2), 200-8; quiz 209.

6. Miller, J. David; Rand, Thomas G.; Jarvis, Bruce B. Medical Mycology (2003), 41(4), 271-291.

7. Nielsen, K. F. Fungal Genetics and Biology (2003), 39, 103- 117.

8. Vining, Leo C. Annual Review of Microbiology (1990), 44, 395-427.

9. Tiebe, Carlo; Huebert, Thomas; Koch, Bernhard; Ritter, Uwe; Stephan, Ina. International Journal for Ion Mobility Spectrometry (2010), 13(1), 17-24.

10. Wallace L, Nelson W, Ziegenfus R, et al. (1991) The Los Angeles TEAM Study: personal exposures, indoor outdoor air concentrations, and breath concentrations of 25 volatile organic compounds. Journal of Exposure Analysis and Environmental Epidemiology 1: 157–192.

11. Kinney PL, Chillrud SN, Ramstrom S, Ross J, and Spengler JD (2002) Exposures to multiple air toxics in New York City. Environmental Health Perspectives 110: 539–546.

12. Walinder R, Norback D, Wessen B, and Venge P (2001) Nasal lavage biomarkers: effects of water damage and microbial growth in an office building. Archives of Environmental Health 56: 30–36.

13. Walinder R, Ernstgard L, Johanson G, Norback D, Venge P, and Wieslander G (2005) Acute effects of a fungal volatile compound. Environmental Health Perspectives 113: 1775–1778.

14. Elke K, Begerow, Oppermann H, Kramer U, Jermann E, and Dunemann L (1999) Determination of selected microbial organic compounds by diffusive sampling and dualcolumn GC-FID – a new feasible approach for the detection of exposure to indoor mould fungi? Journal of Environmental Monitoring: JEM 1: 445–452.

15. Ahearn DG, Price DL, Simmons R, Noble-Wang J, and Crow SA (2004) Indoor moulds and their associations with air distribution systems. Advances in Applied Microbiology 55: 113–138.

16. Tiebe, Carlo; Miessner, Hans; Koch, Bernhard; Huebert, Thomas. Analytical and Bioanalytical Chemistry (2009), 395(7), 2313-2323.

17. Bjurman, Jonny; Nordstrand, Erik; Kristensson, Jan. Indoor Air (1997), 7(1), 2-7.

18. Wilkins, K.; Nielsen, E. M.; Wolkoff, P. Indoor Air (1997), 7(2), 128-134.

19. Nilsson, T.; Larsen, T. O.; Montanarella, L.; Madsen, J. Oe. Journal of Microbiological Methods (1996), 25(3), 245-255.

20. Fiedler, Klaus; Schutz, Edgar; Geh, Stefan . International Journal of Hygiene and Environmental Health (2001), 204(2-3), 111-121.

21. IOM, *Damp indoor spaces and health, Institute of Medicine, National Academy of Sciences*. 2004, Washington, D.C.: National Academy Press.

22. Wilkins, K.; Nielsen, E. M.; Wolkoff, P. Indoor Air (1997), 7(2), 128-134.

23. Gao, Pengfei; Martin, Jennifer. Applied Occupational and Environmental Hygiene (2002), 17(6), 430-436.

24. Tiebe, Carlo; Huebert, Thomas; Koch, Bernhard; Ritter, Uwe; Stephan, Ina. International Journal for Ion Mobility Spectrometry (2010), 13(1), 17-24.

25. Matysik, Silke; Herbarth, Olf; Mueller, Andrea. Journal of Microbiological Methods (2008), 75(2), 182-187.

26. Matysik, Silke; Herbarth, Olf; Mueller, Andrea. Chemosphere (2009), 76(1), 114-119.

27. Bush Robert K; Portnoy Jay M; Saxon Andrew; Terr Abba I; Wood Robert A. The Journal of allergy and clinical immunology (2006), 117(2), 326-33.

28. Polizzi, Viviana; Delmulle, Barbara; Adams, An; Moretti, Antonio; Susca, Antonia; Picco, Anna Maria; Rosseel, Yves; t'Kindt, Ruben; Van Bocxlaer, Jan; De Kimpe, Norbert; et al Journal of Environmental Monitoring (2009), 11(10), 1849-1858.

29. Woolfenden, Elizabeth; Broadway, Graham Special Publication - Royal Society of Chemistry (1992), 108(Clean Air Work), 207-9

30. Kern, H.; Kirshen, N. A. Special Publication - Royal Society of Chemistry (1992), 108(Clean Air Work), 210-12

31. White, Thomas J.; Bruns, Tom; Lee, S.; Taylor, J. Edited by Innis, Michael A. PCR Protocols.: A Guide to Methods and Appl. (1990), 315-22.

32. Compendium of Methods for the Determination of Toxic Organic Compounds in Ambient Air. Center for Environmental Research Information. Office of Research and Development. U.S. Environmental Protection Agency. Cincinnati, OH 45268. January 1999

33. Relman, D. A. 2002. Mining the natural world for new pathogens. Am J Trop Med Hyg 67: 133-4

34. Relman. D.A. 2002. The human body as microbial observatory. Nat Gent 30: 131-3

35. Sunesson, Anna-Lena; Nilsson, Carl-Axel; Andersson, Barbro; Blomquist, Goeran. Annals of Occupational Hygiene (1996), 40(4), 397-410.

36. Hodgson M J; Morey P; Leung W Y; Morrow L; Miller D; Jarvis B B; Robbins H; Halsey J F; Storey E. Journal of occupational and environmental medicine / American College of Occupational and Environmental Medicine (1998), 40(3), 241-9.

37. Johanning E; Biagini R; Hull D; Morey P; Jarvis B; Landsbergis P. International archives of occupational and environmental health (1996), 68(4), 207-18.

38. Walinder, Robert; Ernstgard, Lena; Norbaeck, Dan; Wieslander, Gunilla; Johanson, Gunnar. Toxicology Letters (2008), 181(3), 141-147.

39. Nguyen T L; Gruenke L D; Castagnoli N Jr. Journal of medicinal chemistry (1979), 22(3), 259-63.

40. Fischer S; Weber P C. Biomedical mass spectrometry (1985), 12(9), 470-6.

41. Barron MS, Sutton DA, Veve R, Rinaldi M, Thompson E, Cagnoni PJ, Madinget NE. Interscience Conference on Antimicrobial Agents and Chemotherapy. 2002 Sep 27-30; abstract no. M-870.

42. Kimura, M.; Tokai, T,; Takahashi-Ando, N.; Ohsato, S.; Fujimura, M.; Bioscience, Biotechnology, and Biochemistry. Vol. 71 (2007), No 9 pp 2105-2123.

43. Chiba S, Okada S, Suzuki Y, Watanuki Z, Mitsuishi Y, Igusa R, Sekii T, Uchiyama B. Internal Med. 2009;48(5):363-7.

APPENDIX A

A.1 Mercapturic Acid Conjugates of Glyceollins

A.1.1 Oxygenated mercapturic acid conjugates of glyceollins

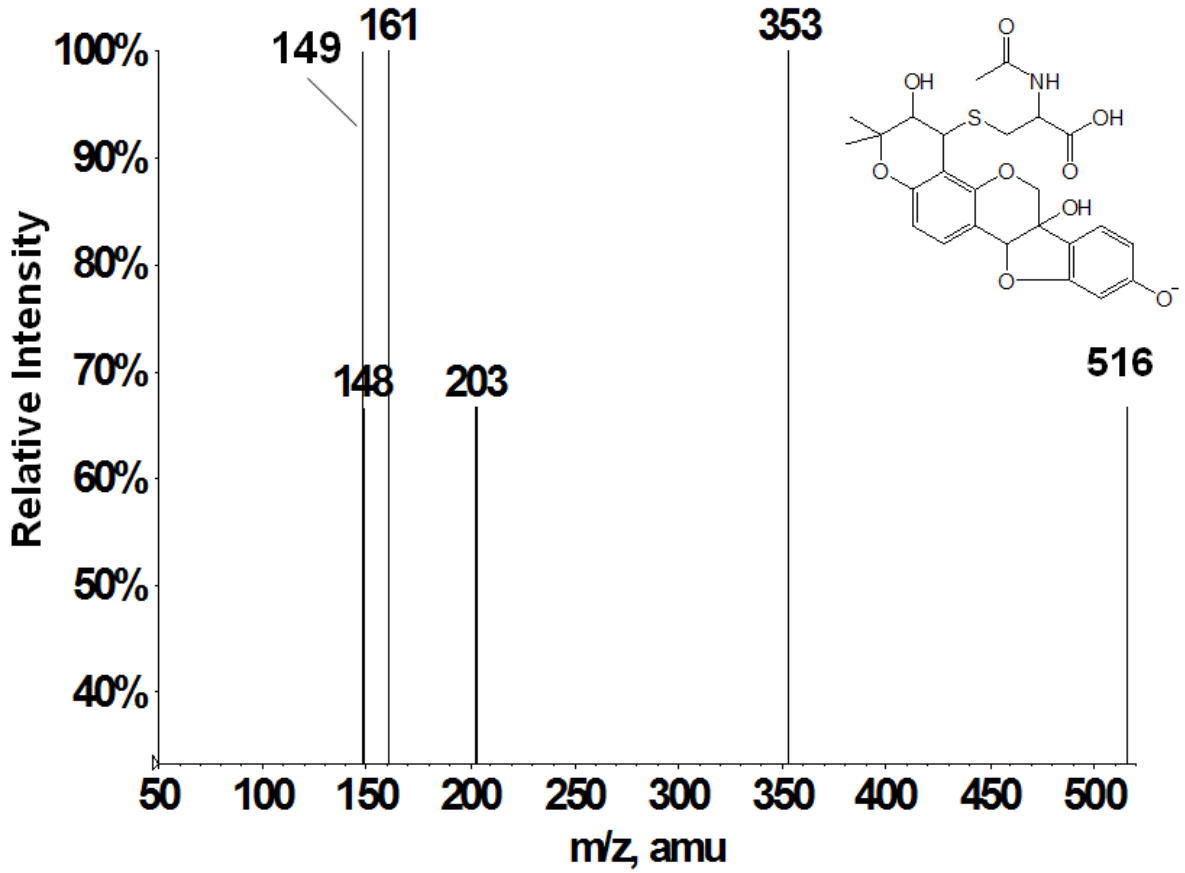

Figure A-1: LC-ESI-MS/MS product ion spectrum of *m/z* 516 precursor in negative ion mode

A.1.2 Mercapturic Acid conjugates of glyceollins

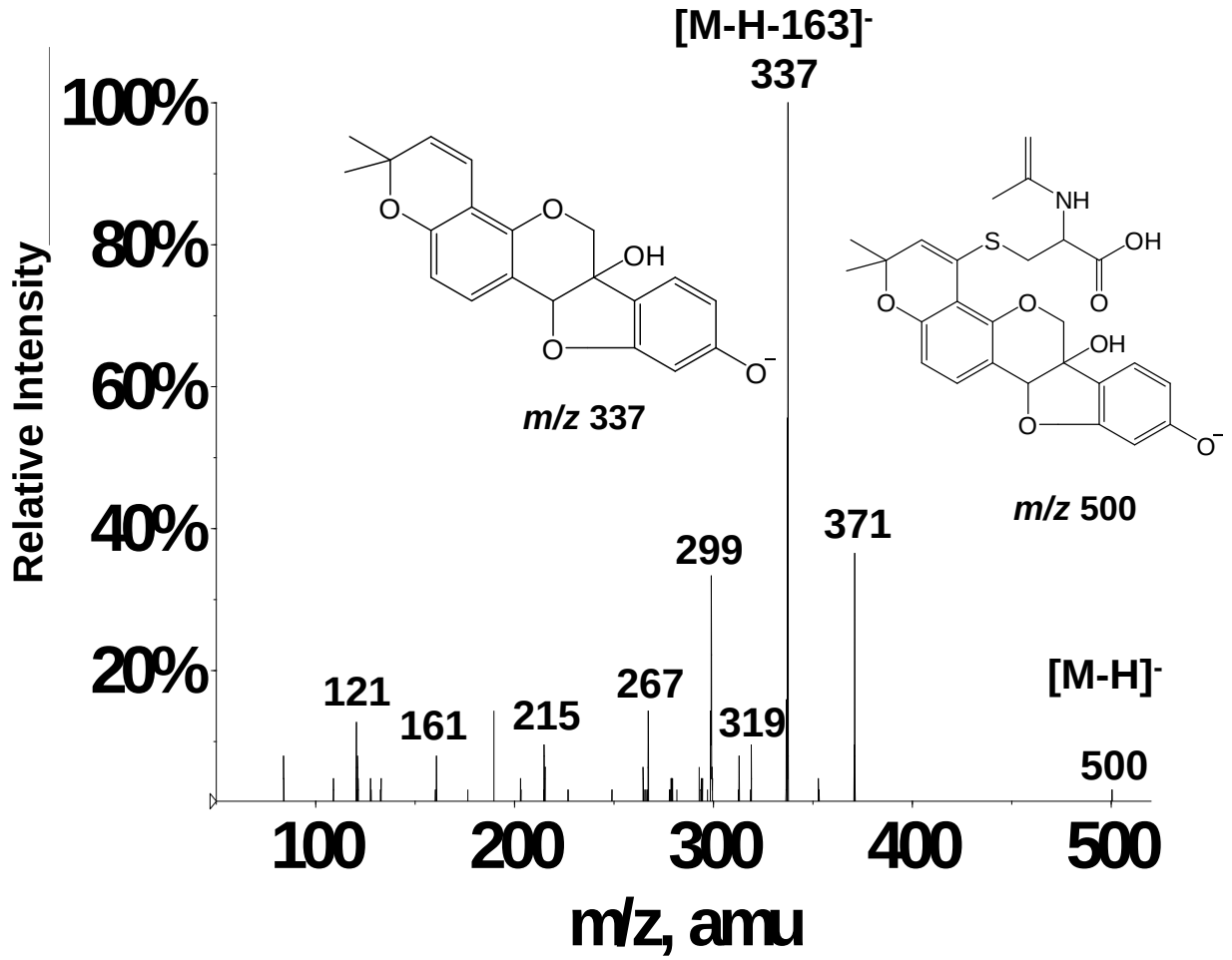

Figure A-2: LC-ESI-MS/MS product ion spectrum of *m/z* 500 precursor in negative ion mode

APPENDIX B

B.1 MVOC Analysis Setup

B.1.1 Experimental Setup

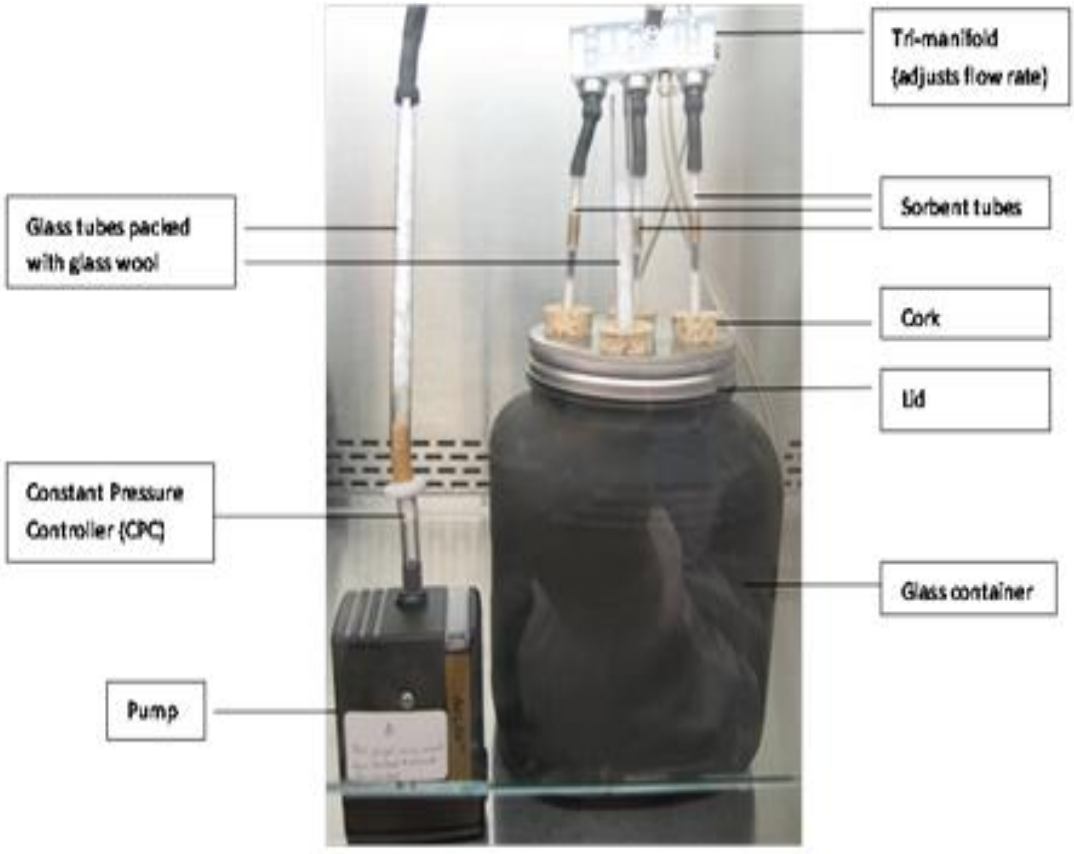

Figure B-1: Schematics of Air Sampling Setup

B.1.2 Photos of drywall fungal growth

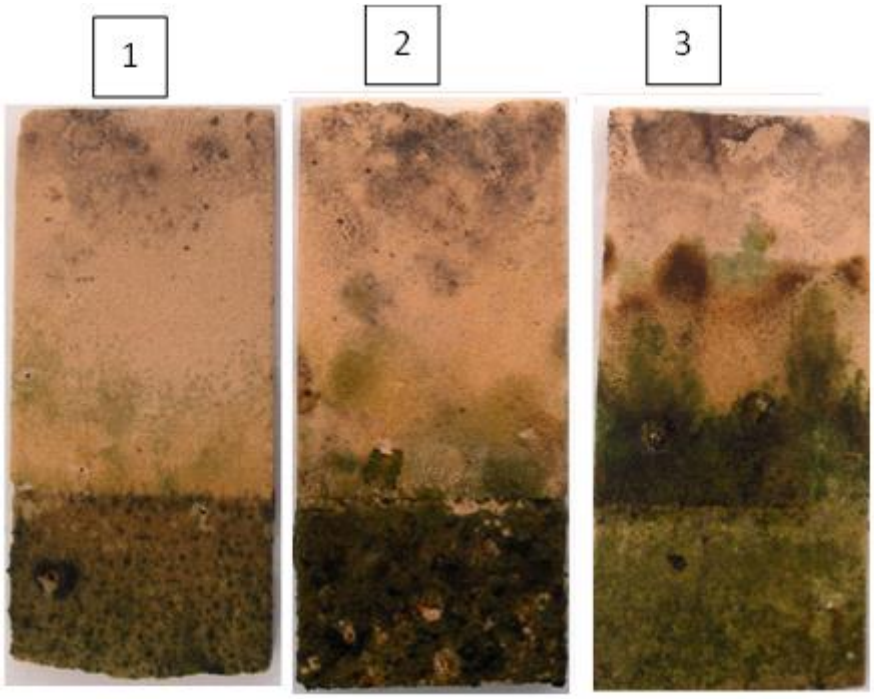

Figure B-2: Pictures of drywall obtained at the end of the experiment from (1) freshwater (2) brackish water and (3) freshwater with added plant food simulated flooding enviornments.

B.1.3 Photos of lab cultivated fungi

B.1.3.1 *Cladosporium sp.*

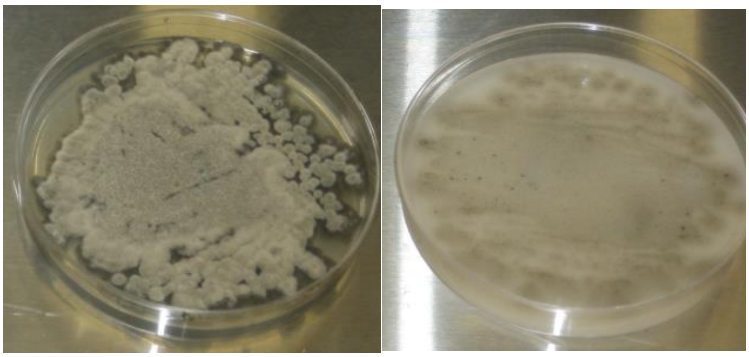

Figure B-3: *Cladosporium* sp. growth on PDA (left) and drywall (right) media after 20 days of cultivation.

B.1.3.2 *Chaetomium sp.*

.

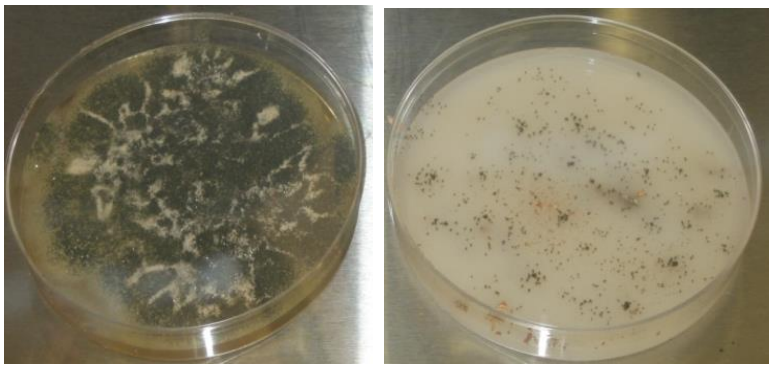

Figure B-4: *Chaetomium sp.* growth on PDA (left) and drywall (right) media after 20 days of cultivation

B.2 Gel Electrophoresis

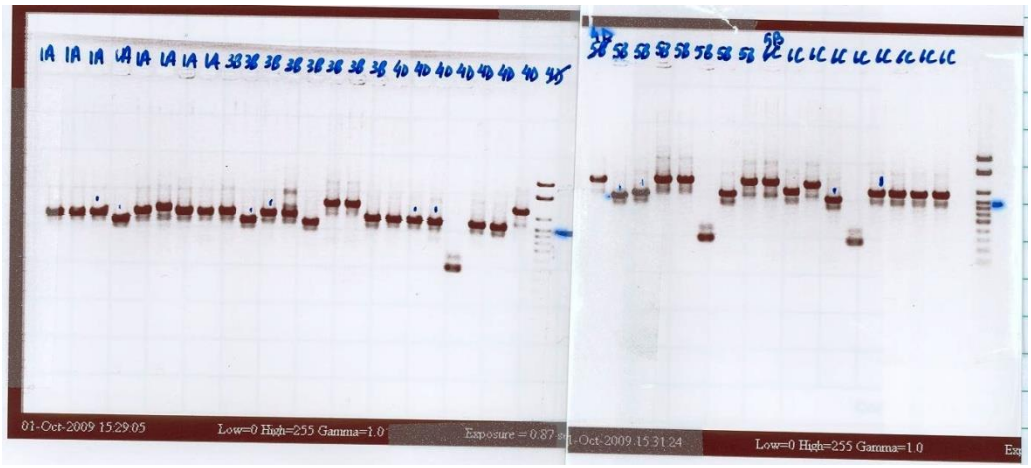

Figure B-5: Stained gel photograph taken after the whole cell PCR of fungal samples that were obtained on Day 70 of the simulated flooding.

B.3 El-Mass Spectra and Decomposition Mechanisms

B.3.1 Mass Spectrum and Decomposition mechanism of 3,3,5-Trimethycyclohenanone

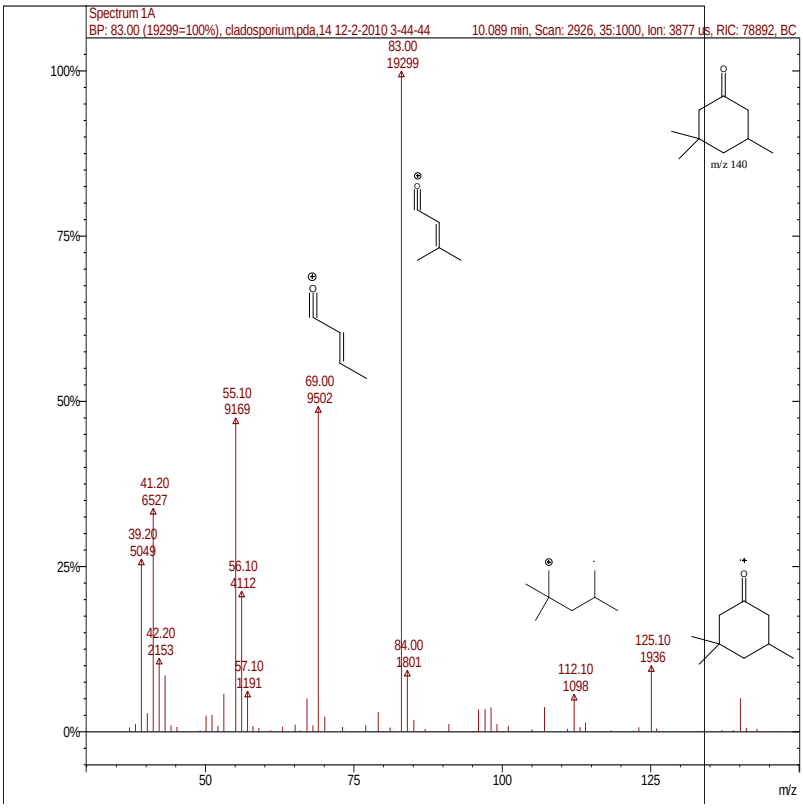

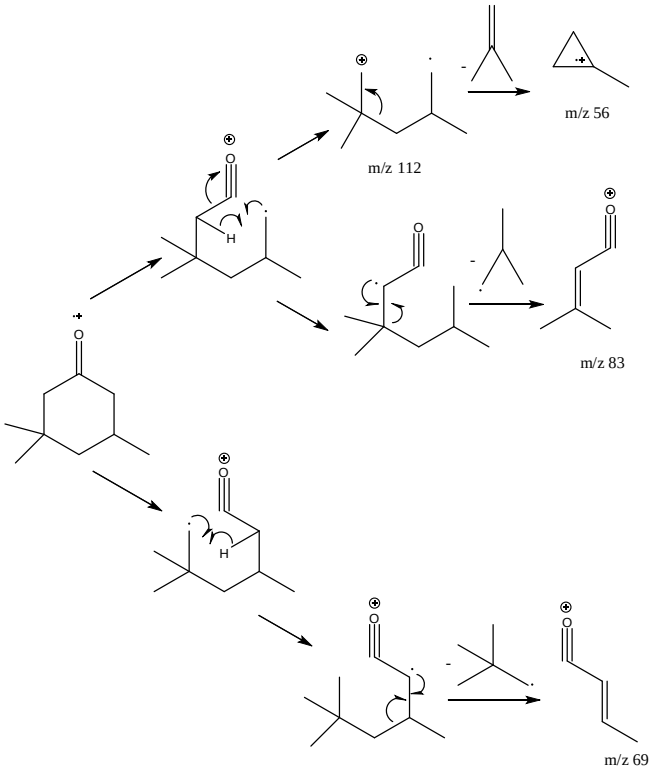

B.3.2 Mass Spectrum and Decomposition mechanism of 2,26-Trimethycyclohenanone

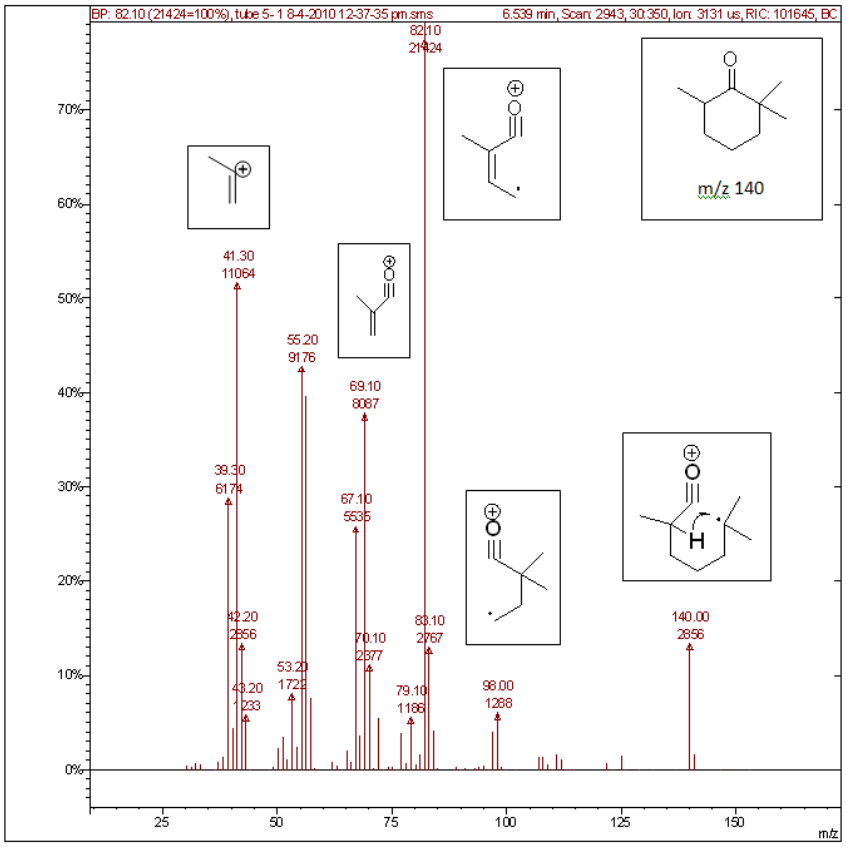

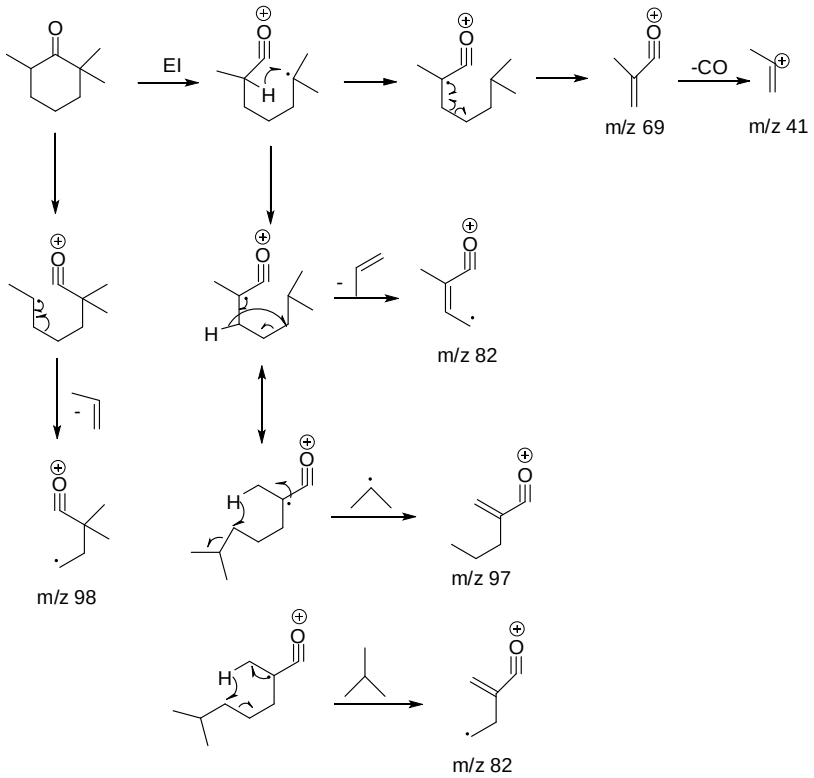

B.3.3 Decompostion Mechanism of 3-octanol

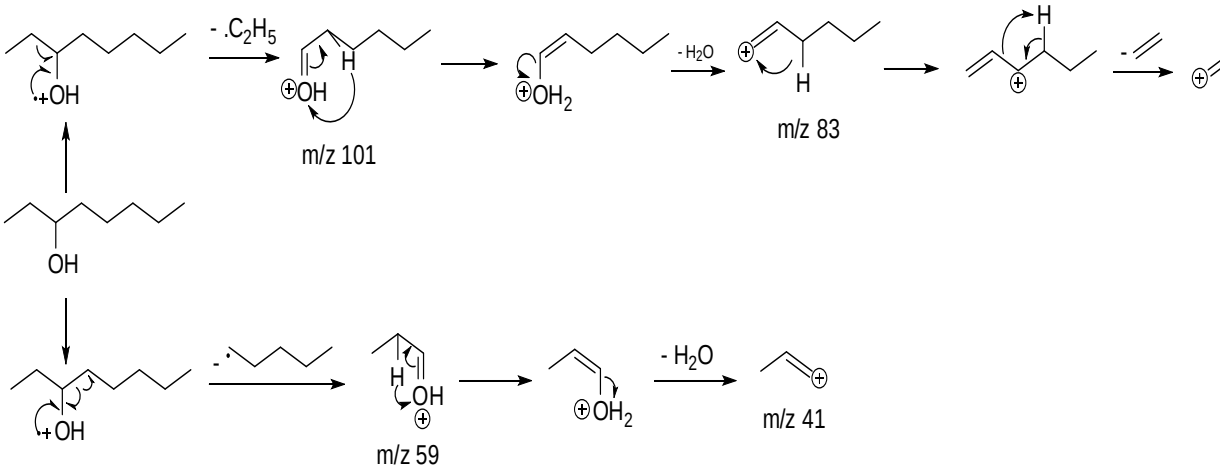

APPENDIX C

C.1 Letters of Approval

XAVIER UNIVERSITY OF LOUISIANA
COLLEGE OF PHARMACY
DIVISION OF BASIC PHARMACEUTICAL SCIENCES
1 Drexel Drive
New Orleans, Louisiana 70125-1098
(504) 520-7432 • Fax: (504) 520-7954

James Payne, PhD
Provost and Executive Director
Graduate School
University of New Orleans
2000 Lakeshore Drive
New Orleans, LA 70148

April 29, 2013

RE: Dissertation Approval Letter on behalf of Ms. Syeda Quadri, Graduate Student in Chemistry

Dear Dr. Payne,

I approve of the use of our collaborative work, pertaining to the metabolism and analysis of glyceollins, in Ms. Syeda Quadri's dissertation. Our efforts resulted in Ms. Quadri's primary authorship of the following publication in the journal, Analytical Chemistry: "Screening and Identification of Glyceollins and Their Metabolites by Electrospray Ionization Tandem Mass Spectrometry with Precursor Ion Scanning." I am pleased that she and Dr. Cole chose to include this work in her dissertation.

Sincerely,

Robert Stratford
Assistant Professor
College of Pharmacy
Xavier University of Louisiana
1 Drexel Drive
New Orleans, LA 70130

USDA
United States Department of Agriculture
Research, Education, and Economics
Agricultural Research Service

August 12, 2011

James Payne, PhD
Provost and Executive Director
Graduate School
University of New Orleans
2000 Lakeshore Dr
New Orleans, LA 70148

RE: Dissertation Approval Letter on behalf of Ms. Syeda Quadri, Graduate Student in Chemistry

Dear Dr. Payne,

I give approval for the use of our collaborative research in Ms. Syeda Quadri's dissertation. Our research resulted in the publication, "Screening and Identification of the Glyceollins and Their Metabolites by Electrospray Ionization Mass Spectrometry", with Ms. Quadri as lead author. Let me know if I can be of further help.

Stephen M. Boue
Research Chemist
Food Processing and Sensory Quality Unit

VITA

The author graduated from Andrew Jackson Fundamental Magnet High School in May 2003. She obtained her Bachelor's degrees in Biology and Chemistry from the University of New Orleans in 2007. In the fall of 2008, she joined the graduate program the University of New Orleans to pursue a Doctorate of Philosophy in Analytical Chemistry. Her graduate research was supervised by Professor Richard B. Cole.